Cretaceous Research 77 (2017) 102–123

Contents lists available at ScienceDirect

Cretaceous Research

journal homepage: www.elsevier.com/locate/CretRes

Integrated biostratigraphy and palaeoenvironmental interpretation of the Upper Cretaceous to Paleocene succession in the northern Moldavidian Domain (Eastern Carpathians, Romania)

Daniel Ţabără [a, *], Hamid Slimani [b], Silvia Mare [a], Carmen Mariana Chira [c]

[a] "Al. I. Cuza" University of Iaşi, Department of Geology, 20A Carol I Blv., 700505 Iaşi, Romania
[b] Scientific Institute, Laboratory of Geology and Remote Sensing, URAC 46, University Mohammed V of Rabat, Avenue Ibn Batouta, P.B. 703, 10106 Rabat-Agdal, Morocco
[c] Babeş-Bolyai University, Department of Geology, M. Kogălniceanu 1, 400084 Cluj Napoca, Romania

ARTICLE INFO

Article history:
Received 6 January 2017
Accepted in revised form 27 April 2017
Available online 10 May 2017

Keywords:
Dinocysts
Calcareous nannofossils
Foraminifera
Cretaceous–Paleogene (K–Pg) succession
Eastern Carpathians

ABSTRACT

This study of the upper Maastrichtian to Danian sedimentary succession from the northern part of the Romanian Eastern Carpathians (Varniţa section) aims to establish an integrated biostratigraphy based on calcareous nannofossils, organic-walled dinoflagellate cysts (dinocysts) and foraminiferal assemblages, and to reconstruct the depositional environments of the interval. The stratigraphic record across the studied section is incomplete, considering that an approximately 16 m thick strata interval from the top of the Maastrichtian to lowermost Danian cannot be analyzed due to a landslide covering the outcrop. The upper Maastrichtian is marked by a succession of biostratigraphic events, such as the First Appearance Datum (FAD) of the nannoplankton taxon *Nephrolithus frequens* and FAD of the dinocyst species *Deflandrea galeata* and *Disphaerogena carposphaeropsis*, and the Last Appearance Datum (LAD) of *Isabelidinium cooksoniae* in the lower part of the section. These bioevents are followed by the LAD of the *Dinogymnium* spp. and *Palynodinium grallator* dinocyst markers in the top of the Maastrichtian deposits analyzed. In terms of foraminiferal biostratigraphy, the upper Maastrichtian *Abathomphalus mayaroensis* Zone is documented in the lower part of the studied section. Some bioevents, such as the bloom of the calcareous dinoflagellate genus *Thoracosphaera* and the FAD of the organic-walled dinocysts *Damassadinium californicum*, *Senoniasphaera inornata*, *Xenicodinium lubricum* and *X. reticulatum* suggest an early Danian age for the middle part of the section. From the Danian deposits in the Varniţa section, we describe a new organic-walled dinocyst species, *Pentadinium darmirae* sp. nov., which is until now the only species of the *Pentadinium* genus discovered in the Paleocene. The occurrence of the global Danian dinocyst marker *Senoniasphaera inornata* in the top of the section, suggests an age not younger than middle Danian (62.6 Ma) for the analyzed deposits.

The palynofacies constituents, as well as the agglutinated foraminiferal morphogroups, used to reconstruct the depositional environments, show that the late Maastrichtian sediments were deposited in an outer shelf to distal (bathyal) environment, followed by a marine transgression during the Danian.

1. Introduction

Numerous paleontological studies have revealed a major mass extinction at the Cretaceous–Paleogene (K–Pg) boundary. This global extinction event of most of the marine and terrestrial biota at the end of the Cretaceous is supposed to be caused by an asteroid impact (Alvarez et al., 1980), intense volcanic activity from western India (Keller, 2008; Keller et al., 2009) or climatic changes (Courtillot et al., 1986; Courtillot, 1990).

Many groups of organisms such as dinosaurs and ammonites suffered a mass extinction at the K–Pg boundary. An important decline is also shown by the marine microfossils such as planktonic foraminifera and calcareous nannoplankton (Paul, 2005; Twitchett, 2006; Westerhold et al., 2008), while deep-water benthic foraminifers, radiolarians and organic-walled dinoflagellate cysts were less affected by the crisis (Hansen, 1977; Brinkhuis and Zachariasse,

* Corresponding author.
E-mail addresses: dan.tabara@yahoo.com (D. Ţabără), h_slimani@yahoo.com (H. Slimani), silvia_mare@yahoo.com (S. Mare), carmen.chira@ubbcluj.ro (C.M. Chira).

http://dx.doi.org/10.1016/j.cretres.2017.04.021
0195-6671/

1988; Hollis, 1996; Coccioni and Marsili, 2007; Slimani et al., 2010; Machalski et al., 2016).

The Maastrichtian–early Paleocene foraminiferal assemblages from the central and northern parts of the Moldavidian Units, Eastern Carpathians, were studied by Ionesi and Tocorjescu (1968), Ionesi (1966, 1975), Ion et al. (1982) and Guerrera et al. (2012). The Maastrichtian assemblage is mainly composed of various taxa of calcareous foraminifera, such as *Abathomphalus mayaroensis* and *Globotruncana* spp., and agglutinated foraminifera, e.g. *Caudammina ovula*, *Rzehakina inclusa*, *Spiroplectammina spectabilis*. Among the Danian taxa, mainly agglutinated foraminifera were identified, an biostratigraphic marker being *Rzehakina fissistomata* according to the authors listed above.

From the same Moldavidian tectonic units, some palynological results at the K–Pg transition were presented by Olaru (1978). The author noted that in the Maastrichtian, the Normapolles group (primitive angiosperms) dominates the palynological assemblages (65–70%), spores and dinocysts being less abundant. The Paleocene microflora shows a decline of the Normapolles group, the prevalent taxa being the mono- and dicotyledonous angiosperms, as well as some pteridophytes and gymnosperms. As to the relative frequency of the dinoflagellate cysts, Olaru (1978) records a decrease in the Paleocene marine assemblages, compared to those identified in Maastrichtian deposits. In the Campanian–Paleocene stratigraphic interval of the Eastern Carpathians, Antonescu and Alexandrescu (1979) established four dinocyst zones, namely: the *Cerodinium diebelii – Palaeocystodinium golzowense* Zone (upper Campanian–lower Maastrichtian), *Deflandrea druggi* Zone (upper Maastrichtian), *Trithyrodinium evittii – Cerodinium striatum* Zone (Danian) and *Cerodinium speciosum – Deflandrea* cf. *oebisfeldensis* Zone (Thanetian). The first two zones were identified in the Hangu Formation, the third zone in the uppermost 10 m of the Hangu Formation, in the Runcu Formation and the lower part of the Izvor Formation, while the fourth zone was recorded in the Izvor Formation.

Other biostratigraphical studies of the K–Pg boundary are based on calcareous nannofossil assemblages from the south-western part of the Eastern Carpathians. In the Ialomiţa Valley section, Melinte and Jipa (2005), Bojar et al. (2009) and Bojar and Bojar (2013) identified an uppermost Maastrichtian mass extinction of the calcareous nannoplankton, followed by some earliest Danian bioevents represented by two extensive blooms, one a calcareous dinocyst genus *Thoracosphaera*, and one of the nannofloral species *Braarudosphaera bigelowii*. In the northern part of Eastern Carpathians, Ionesi (1997) recorded a Paleocene calcareous nannoplankton assemblage from the Runcu Formation, with *Ellipsolithus macellus* indicating the NP4 Zone (late Danian).

The aims of the present paper comprise: (1) the establishment of the stratigraphic distribution of dinocysts, calcareous nannoplankton and plaktonic and benthic foraminifera from the Varniţa section; (2) a detailed biostratigraphical interpretation of the upper Maastrichtian to Danian sedimentary succession, based on these micropaleontological assemblages, and (3) the evaluation of the palaeoenvironmental conditions based on palynofacies characteristics and the microfossil taxa.

2. Geological setting

The Eastern Carpathians represent a segment, over 600 km long, of the Carpathian tectonic chain, composed mainly of Jurassic to Miocene deposits. According to Săndulescu (1984), the Carpathian chain in Romania resulted from a collision between the African-Arabic and European plates, which led to the gradual closure of the Tethys Ocean during the Cretaceous and Miocene convergence events. The deformation in the Romanian Carpathians took place in two stages (Săndulescu, 1984): in the Cretaceous, when the Transylvanide and Dacide Units were build up; and during the Miocene, when the Moldavidian Unit in the Eastern Carpathians was formed. The Moldavidian Unit is divided, from west to east, into the Inner Moldavides (the Teleajen, Macla and Audia nappes), consisting mainly of Cretaceous deposits, and the Outer Moldavides (the Tarcău, Vrancea and the Pericarpathian nappes) comprising Cretaceous to early Miocene "flysch" deposits (Săndulescu, 1984; Grasu et al., 1988; Bădescu, 2005) (Fig. 1C).

The geological cross section analyzed in this paper is located in the eastern part of the Tarcău Nappe (Fig. 1A), more precisely on the Varniţa river, 2 km southwest of the Gura Humorului city. The Cretaceous–Paleocene sedimentary succession identified along the river was assigned to three geological formations, namely the Hangu, Runcu and Izvor formations (Ionesi and Tocorjescu, 1968; Ionesi, 1971; Ionesi, 1997).

The Hangu Formation (~800 m thick), of which we analyzed only the upper part (about 23 m in thickness; Fig. 2), is characterized by an alternation of marlstones with fucoids, claystones (30–70 cm thick), sandy limestones (40–60 cm thick) and calcarenites (up to 90 cm thick). The fucoids mostly belong to *Chondrites intricatus* (Bojar and Bojar, 2013), possibly indicating an anoxic environment (Uchman, 2004). The calcarenites sometimes show calcite diaclases. In the study section, these deposits lie in normal position with a southwest inclination of approximately 60° (Fig. 1A). The top of the Hangu Formation contains debris-flow deposits, some 1 m thick, consisting of black unstratified shales with marlstone lithoclasts derived from older Cretaceous deposits (Fig. 2C).

Upwards, the succession continues with the Runcu Formation (~15 m thick, according to Ionesi, 1997), which does not outcrop completely in the study area because of partial cover by a landslide. The formation is composed of debris-flow deposits (Ionesi, 1997) consisting mainly of black shales matrix mixed with greenish claystones without stratification (Fig. 2A). This matrix of pelitic rocks contains thin intercalations of quartzarenites, reddish fine sandstones, as well as some reworked lithoclasts of marlstones and sandstones derived from the Cretaceous (Audia and Hangu formations). The black shales encountered in the Runcu Formation also are reworked from the Audia Formation (Ionesi, 1997). Guerrera et al. (2012) interpreted the lithologic interval assigned to the Runcu Formation as a slumped body (olistostrome) deposited on the continental slope.

The Runcu Formation is followed by the Izvor Formation, consisting mainly of turbiditic deposits represented by laminated black shales (20–100 cm thick), greenish claystones and calcarenite interlayers (15–110 cm thick). In the studied section, only the lower part, some 35 m thick of the formation, was identified. According to our observations, these deposits show a reverse position, due to strong folding of the area.

3. Previous stratigraphic results

Research based on foraminiferal, dinocyst and nannofossil assemblages by various authors led to the attribution of some slightly different biostratigraphic dating of the sedimentary units across the Cretaceous–Paleogene succession in the study area.

The upper part of the Hangu Formation in the Varniţa section yielded a foraminiferal assemblage comprising *Abathomphalus mayaroensis*, *Eponides bolli*, *Globotruncana arca*, *G. contusa*, indicating a late Maastrichtian age (Ionesi and Tocorjescu, 1968; Ionesi, 1971). A different opinion concerning the age of this stratigraphic interval (the top of the Hangu Formation, the uppermost 10 m) in the same section was advanced by Antonescu and Alexandrescu (1979), who recorded a dinocyst assemblages with *Cerodinium*

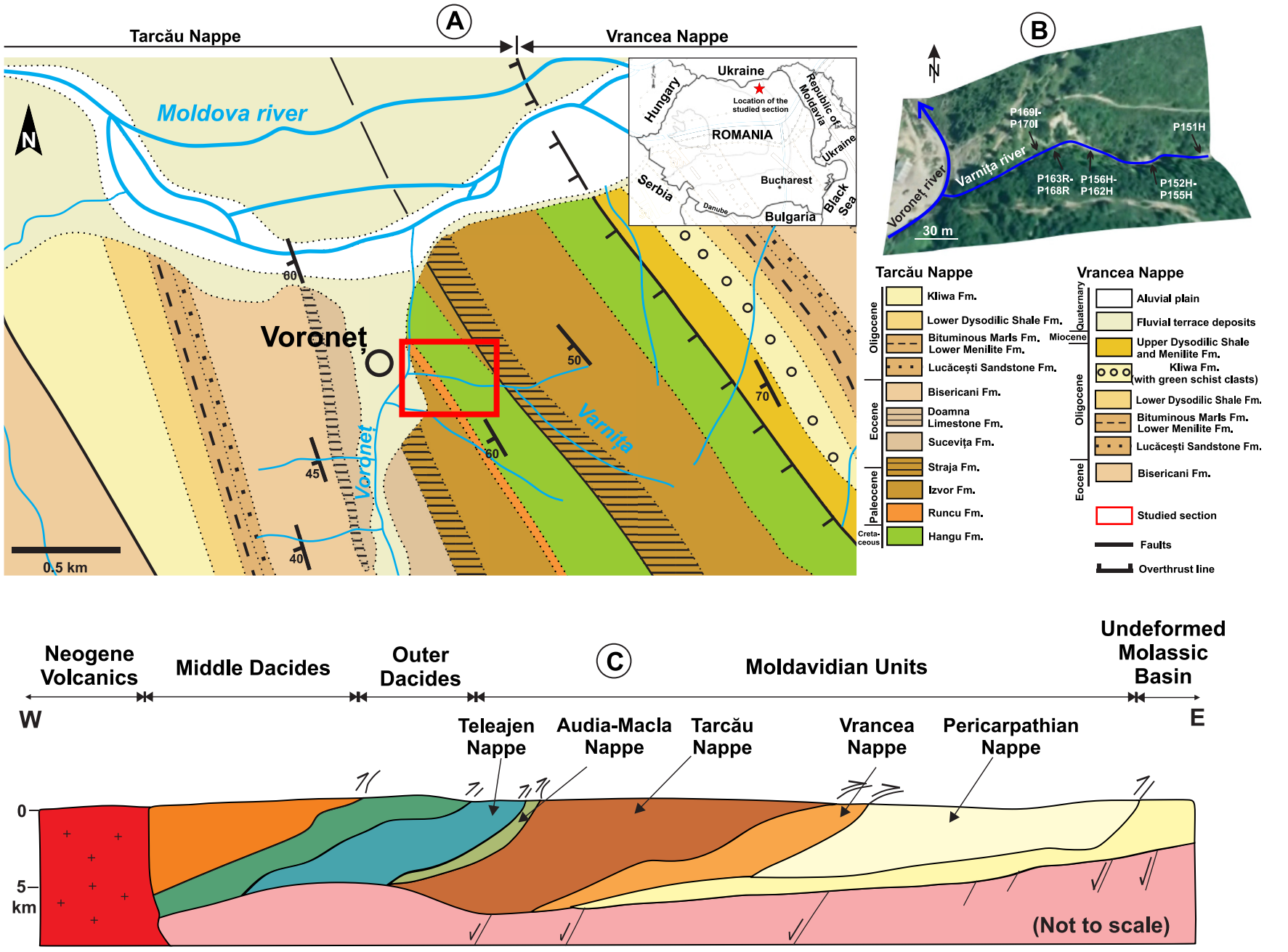

Fig. 1. Geological and geographical setting of the studied Upper Cretaceous–Paleogene interval. **A**. Geological map with location of the studied section (after Ionesi, 1971; modified). **B**. Overview of the Varnița river with sample positions. **C**. Geological cross-section of the Eastern Carpathian Chain (after Bădescu, 2005).

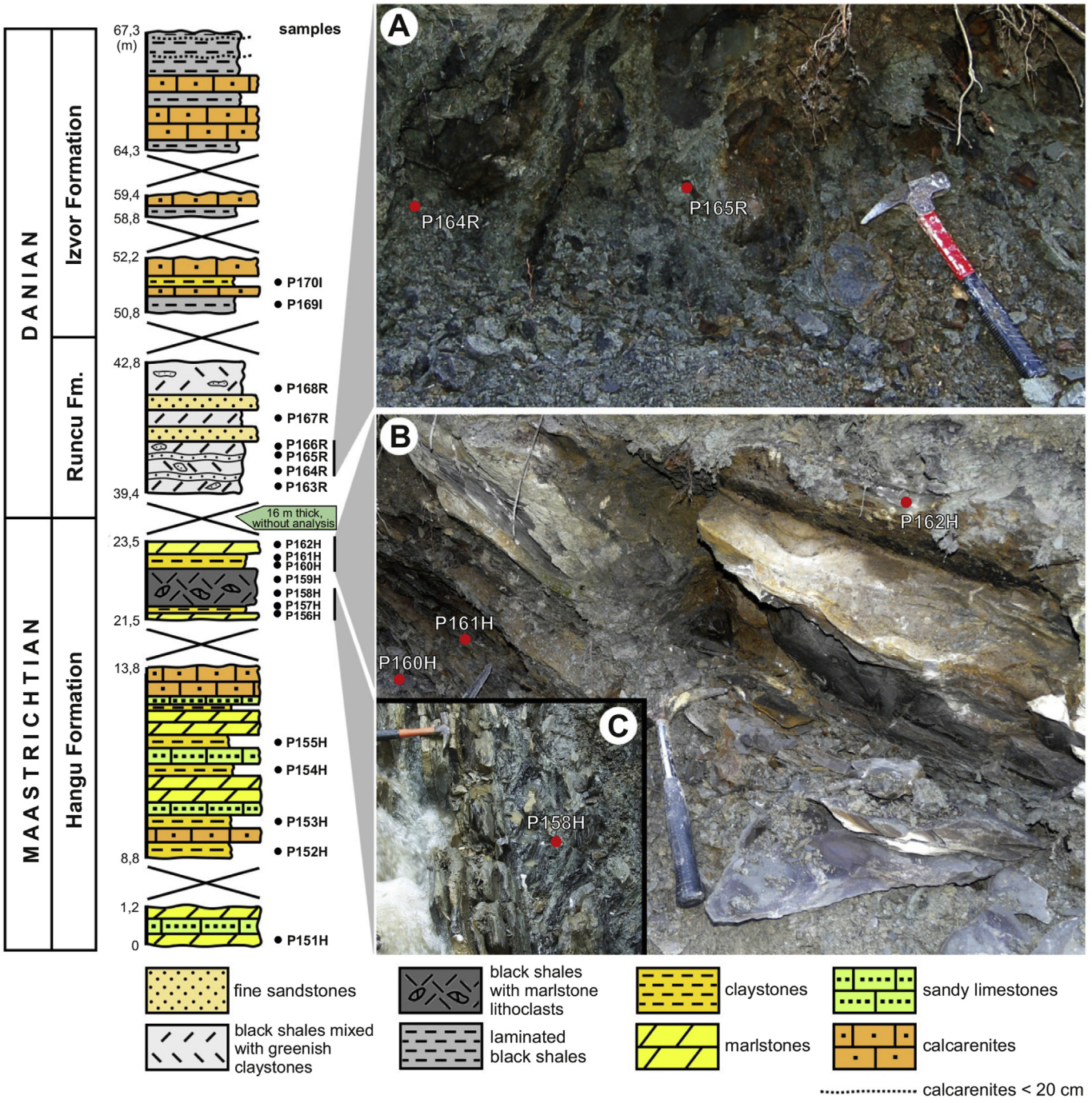

Fig. 2. Stratigraphic succession of the Varniţa section. **A**. Reworked black shales matrix mixed with greenish claystones (Runcu Formation). **B**. Alternation of claystones and marlstones in the top of the Hangu Formation. **C**. Debris-flow deposits (right side of the picture) consisting of black shales without stratification, with marlstone lithoclasts.

striatum, *Deflandrea druggi*, *Senoniasphaera inornata*, indicating a Danian age. According to Bojar and Bojar (2013), the K–Pg boundary on the Varniţa river has been identified in the uppermost part of the Hangu Formation. These authors recorded a calcareous nannoplankton assemblages dominated by *Micula* spp. and *Watznaueria barnesae* (70–90% of the total assemblages) within the 145 cm thick interval just below the K–Pg boundary, a bloom of *Thoracosphaera*, a drop in frequency for *Micula* and *W. barnesae* and the first occurrence of *Neobiscutum parvulum* (NP1 Zone) above the boundary. In the Varniţa section, the negative excursion of the $\delta^{13}C$ values of organic material, typical for the lowermost Danian, was not recorded (Bojar and Bojar, 2013). Unfortunately, the K–Pg boundary has not been well located in the Varniţa section by Bojar and Bojar (2013), to allow a correlation with our biostratigraphical data from the same outcrop.

The age of the Runcu Formation (Varniţa section) was established based on calcareous nannoplankton (Ionesi, 1997), including *Chiasmolithus danicus*, *Cruciplacolithus tenuis* and *Ellipsolithus macellus* (NP4 Zone, upper Danian). The Danian–Thanetian age of the Runcu Formation was supported by the dinocyst assemblages (Antonescu and Alexandrescu, 1979).

Until now, two different opinions concerning the age of the lower part of the Izvor Formation (Varniţa section) were advanced. Ionesi and Tocorjescu (1968) and Ionesi (1971) suggest a Danian age based on agglutinated foraminifera (*Glomospira diffundens*, *Haplophragmoides glomeratus*, *Recurvoides deflexiformis*, *Rzehakina fissistomata*). On the other hand, Antonescu and Alexandrescu (1979) proposed a Thanetian age, based on dinocyst taxa such as *Cerodinium diebelii*, *Cerodinium speciosum* and *Duosphaeridium rugosum*.

4. Material and methods

Twenty samples of the K–Pg succession from the Varniţa section (E 25°52′06,63″, N 47°31′58,84″) were collected for microfossil analysis. The sedimentary succession has a total thickness of 67 m (Fig. 2) and twelve samples (P151H–P162H) were collected from the Hangu Formation, six samples (P163R–P168R) from the Runcu Formation and two samples (P169I, P170I) from the Izvor Formation.

For the palynological and palynofacies analysis, all samples were processed using standard palynological techniques (e.g. Batten, 1999). Approximately 50 g of deposit from each sample were treated with HCl (37%) to remove carbonates and HF (48%) to remove the silicate minerals. Denser particles were separated from the organic residue using $ZnCl_2$ with a density of 2.0 g/cm^3. The palynological residues were mounted on microscopic slides using glycerine jelly. The palynomorphs photomicrographs (Figs. 3–5) were taken with a digital Leica DFC420 camera mounted on a Leica DM1000 microscope. The taxonomy of dinocysts follows Dinoflaj2 (Fensome et al., 2008) and Slimani et al. (2008). Appendix A gives a species list of the dinoflagellate cysts, spores and pollen encountered. All the microscopic slides are stored in the collection of the Geology Department, "Al. I. Cuza" University of Iaşi.

For the palynofacies analysis, at least 300–400 of un-oxidized particles were counted in each sample, these being included at the three main groups of kerogen constituents proposed by Tyson (1995), Bombardiere and Gorin (2000), Mendonça Filho et al. (2002), Carvalho et al. (2006) and Ţabără et al. (2015), namely: the phytoclasts group (opaque and translucent organic particles derived from terrestrial plants), the palynomorphs group, and the Amorphous Organic Matter (AOM) group which includes structureless organic components derived from phytoplankton (granular AOM) or degraded higher plant debris (gelified AOM).

For a detailed palaeoenvironmental analysis (proximal-distal trends) the following interpretive parameters based on palynofacies observations (all ratios are expressed in decimal logarithms; Tyson, 1995) were used:

(i) the ratio of opaque to translucent phytoclasts (O:Trans). According to Tyson (1995) and Carvalho et al. (2013), translucent particles are deposited in nearshore environments. In contrast, opaque phytoclasts are derived from the oxidation of translucent particles that have suffered a transport over a prolonged period of time. The ratio tends to increase distally and can be used to interpret proximal-distal trends (Steffen and Gorin, 1993). Generally, high values of opaque and translucent phytoclasts are deposited by rivers in deltaic environments (Tyson, 1995), however large amounts of phytoclasts can also occur in deep waters, transported by turbidity currents (Habib, 1982; Carvalho et al., 2013).

(ii) the continental/marine palynomorphs ratio (C/M). The ratio can also be used as an indicator of proximal-distal trends (Pellaton and Gorin, 2005), and is calculated by the number of all terrestrial palynomorphs (spores + pollen) divided by the number of marine palynomorphs (dinoflagellate cysts). The C/M ratio generally decreases offshore. The relative abundance of palynomorphs was also plotted in a spore-pollen-microplankton (SPM) ternary diagram (Federova, 1977; Duringer and Doubinger, 1985) in order to show onshore-offshore depositional environments and transgressive-regressive trends.

For the study of the benthic and planktonic foraminifera, approximately 150–200 g of deposit from each sample were processed. The separation of microfossils was carried out using the water-immersion and successive decantation method. The total residue obtained by decantation was passed through three sieves (ø – 0.122 mm; 0.263 mm; 0.466 mm), and the microfossils were picked from each fraction using a Carl Zeiss Jena SM XX binocular stereo microscope. The photomicrographs (Fig. 6, 7) were taken with a Vega/Tescan SEM microscope. All identified taxa of foraminifera are listed in Appendix B.

Palaeoenvironment estimates have been deduced using the agglutinated foraminiferal morphogroup method (Nagy et al., 1995; van den Akker et al., 2000; Kaminski and Gradstein, 2005; Cetean et al., 2011; Murray et al., 2011; Setoyama et al., 2011, 2013). The morphogroup analysis assumes that species with different test shape have different habitats and feeding strategies, and variations in the relative abundance of the morphogroups can reflect environmental changes (Corliss, 1985; Jones and Charnock, 1985; Murray et al., 2011).

The morphogroup M1 (tubular forms) is very rare in the shelf environments, but shows an increase in abundance with water depth, reaching the maxima in the middle and lower bathyal zones (Nagy et al., 1995; Kaminski and Gradstein, 2005). M2a (forms with globular chambers) is very common in the bathyal and abyssal environments, while M2b and M2c are more characteristic for shelf to deep marine environments. M3a (flattened trochospiral, planspiral and streptospiral forms) occurs commonly in lagoon to abyssal environments (Nagy et al., 1995), whereas M3b and M3c are characteristic of deep-water environments (Cetean et al., 2011). Regarding the M4 morphogroup, both M4a (rounded planspiral) and M4b (elongated multiserial forms) are commonly found in inner shelf to upper bathyal environments.

The diversity of the agglutinated foraminiferal assemblages was calculated using the PAST software, version 3.14 (Hammer et al., 2001; Hammer and Harper, 2006). Fisher alpha diversity index, as a measure of species diversity in this study, was calculated only for agglutinated foraminifera because the calcareous foraminifera were not identified in the middle and upper part of the studied section, probably due to carbonate dissolution.

The calcareous nannoplankton was analyzed in order to establish the age of the deposits. For the upper Maastrichtian and Danian, the CC calcareous nannofossil biozonation (Sissingh, 1977; Perch-Nielsen, 1985), the UC scheme of Burnett (1998) and the standard Paleogene nannofossil zones (NP) of Martini (1971) were taken into account. The analysis of these microfossils was mainly qualitative. The smear slides prepared from the samples were examined under a light microscope at 1000× magnification (Axioskop 40 Zeiss microscope with PowerShot G10 Cannon digital camera) under plane polarized light and cross polarized light. Some of the most important marker taxa are shown in Fig. 8.

The new organic-walled dinocyst species described in this study is registered in Zoobank under the urn:lsid:zoobank.org:act:3895CBE4-2D33-49A4-B62E-D96B40626D7A.

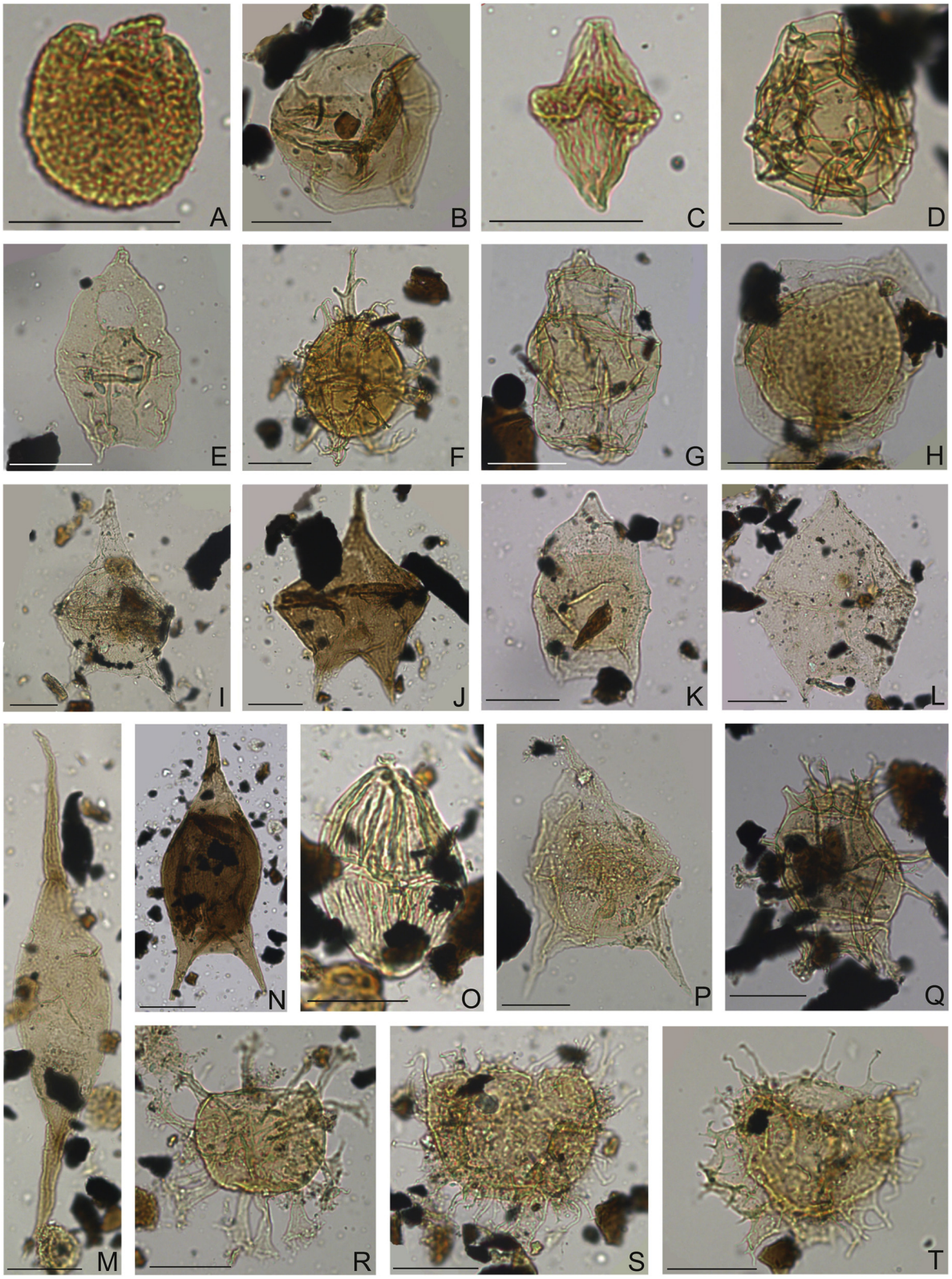

Fig. 3. Selected dinoflagellate cysts from the Hangu Formation (scale bar: 30 μm). A. *Elytrocysta* druggii, sample P151H. B. *Alterbidinium* sp. cf. *A. varium*, P151 (reworked). C. *Dinogymnium acuminatum*, P151H. D. *Pterodinium* cingulatum, P152H. E. *Chatangiella ditissima*? P151H (reworked). F. *Spiniferella cornuta* subsp. *cornuta*, P161H. G. *Hystrichosphaeropsis quasicribrata*, P152H. H. *Leberidocysta chlamydata* subsp. *schiølerii*, P152H. I. *Cerodinium* speciosum, P154H. J. *Phelodinium tricuspis*, P154H. K. *Chatangiella* sp. A of Schiøler and Wilson, 1993, P154H. L. *Palaeoperidinium* pyrophorum, P154H. M. *Palaeocystodinium golzowense*, P154H. N. *Cerodinium* diebelii, P154H. O. *Dinogymnium albertii*, P154H. P. *Deflandrea galeata*, P151H. Q. *Rottnestia wetzelii* subsp. *wetzelii*, P158H. R. *Hystrichosphaeridium tubiferum* subsp. *tubiferum*, P154H. S. *Areoligera senonensis*, P154H. T. *Palynodinium grallator*, P157H.

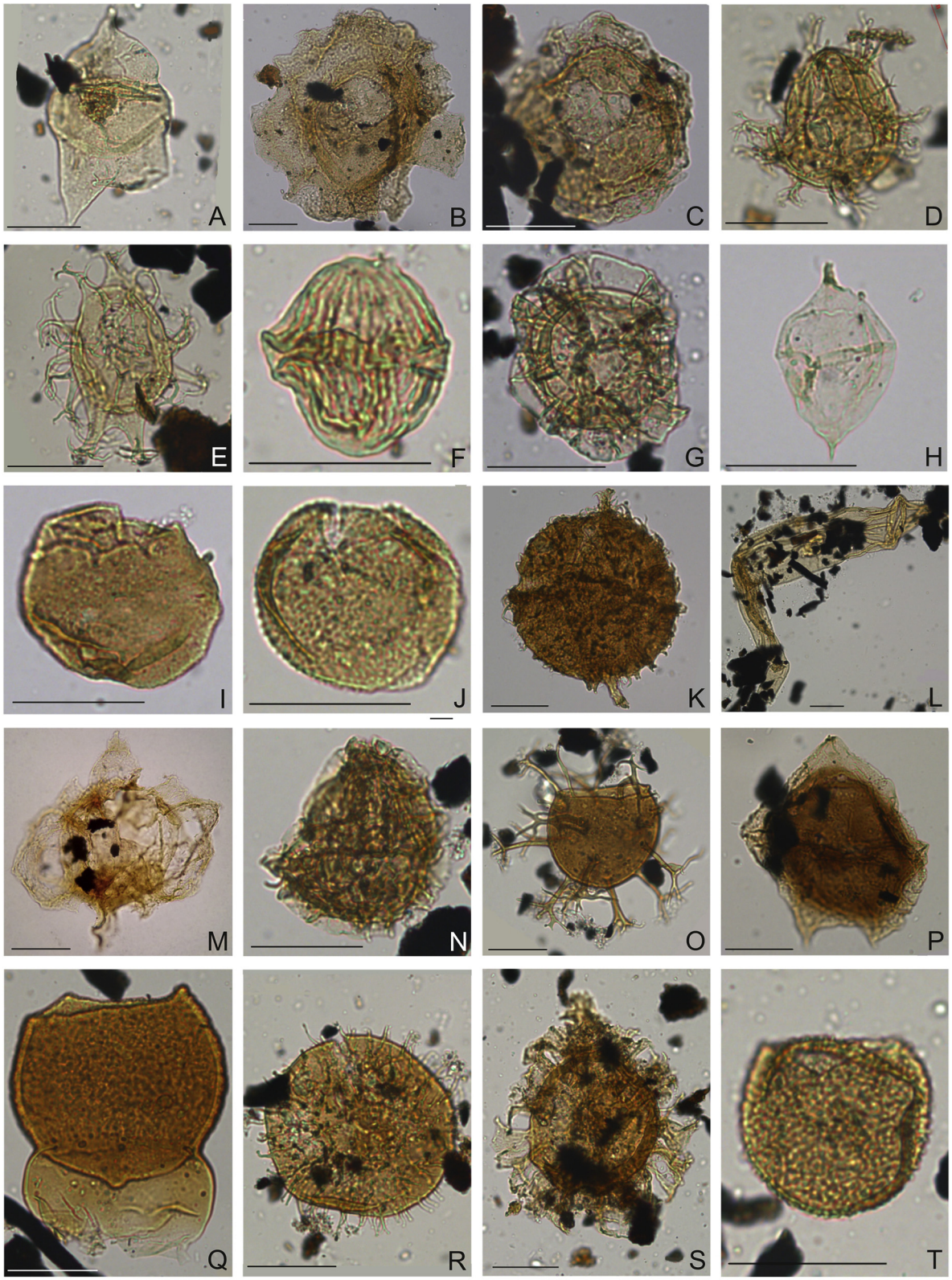

Fig. 4. The late Maastrichtian-Danian dinoflagellate cysts from the Hangu, Runcu and Izvor formations (scale bar: 30 μm). A. *Isabelidinium cooksoniae*, sample P154H. B. *Muratodinium fimbriatum*, P158H. C. *Membranilarnacia polycladiata*, P158H. D. *Spiniferites ramosus* subsp. *ramosus*, P161H. E. *Spiniferites membranaceus*, P161H. F. *Dinogymnium cretaceum*, P161H. G. *Pterodinum cretaceum*, P161H. H. *Diconodinium wilsonii*, P162H. I. *Kallosphaeridium yorubaense*, P164R. J. *Xenicodinium delicatum*, P164R. K. *Fibrocysta licia*, P165R. L. *Yolkinigymnium lanceolatum*, P166R. M. *Disphaerogena carposphaeropsis*, P168R. N. *Xenicodinium reticulatum*, P168R. O. *Achomosphaera regiensis*, P168R. P. *Trithyrodinium evittii*, P169I. Q. *Duosphaeridium rugosum*, P169I. R. *Operculodinium centrocarpum*, P170I. S. *Damassadinium californicum*, P170I. T. *Xenicodinium lubricum*, P170I.

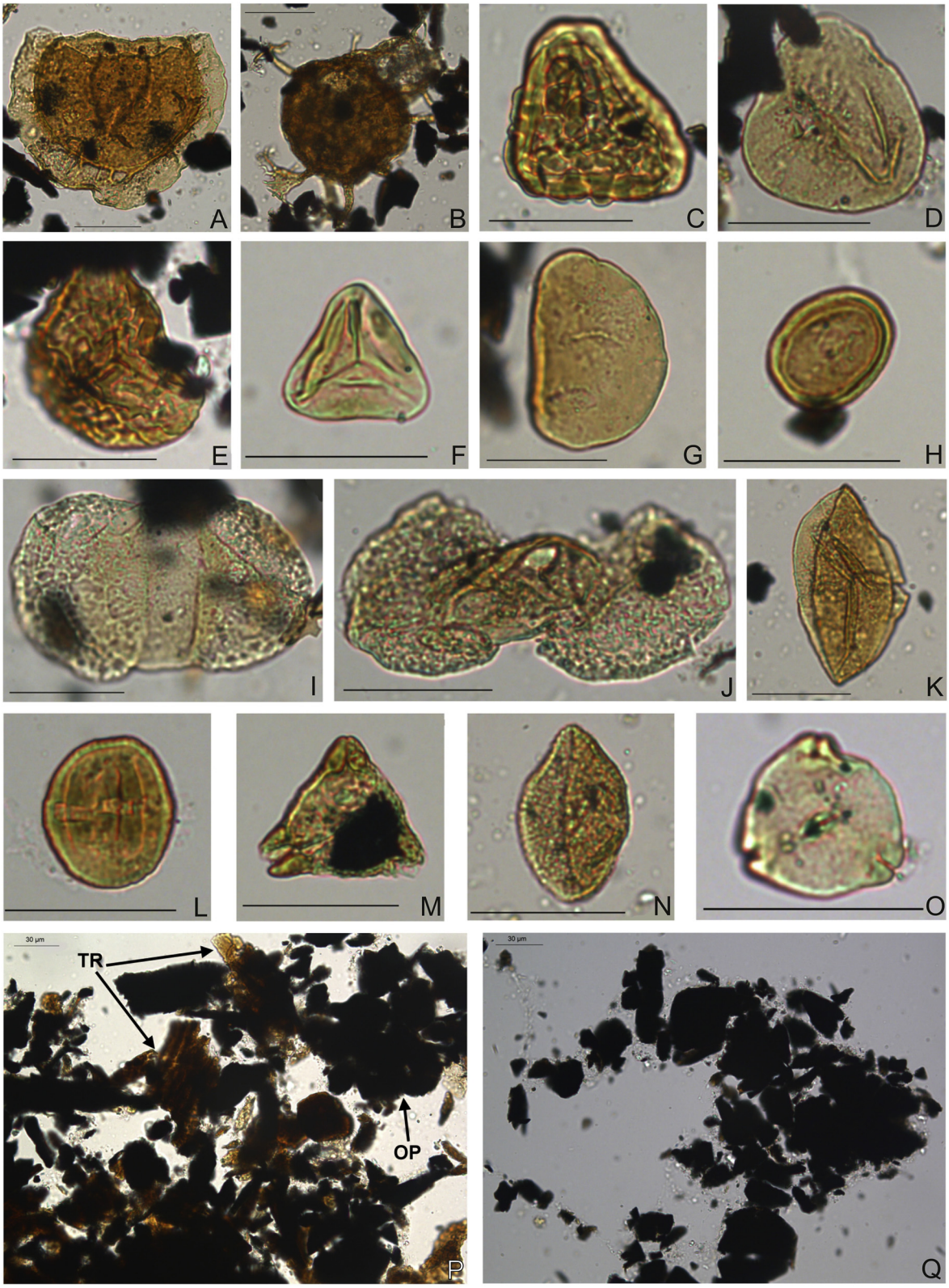

Fig. 5. Dinocyst taxa, continental palynomorphs and particulate organic matter (taken under transmitted white light) from the Hangu, Runcu and Izvor formations (scale bar: 30 µm). A. *Senoniasphaera inornata*, sample P170I. B. *Hafniasphaera graciosa*, P170I. C. *Polypodiaceoisporites* sp., P154H. D. *Deltoidospora australis*, P155H. E. *Camarozonosporites* sp., P156H. F. *Gleicheniidites senonicus*, P157H. G. *Laevigatisporites haardti*, P161H. H. *Classopollis* sp., P157H. I. *Alisporites* sp., P154H. J. *Podocarpidites* sp., P154H. K. *Cycadopites* sp., P170I. L. *Sapotaceoipollenites* sp., P152H. M. *Nudopollis* sp., with framboidal pyrite, P162H. N. *Arecipites* sp., P170I. O. *Myricipites* sp., P162H. P. A mixed assemblage of opaque phytoclasts (OP) and translucent organic particles (TR) (Hangu Formation, P155H). Q. Palynofacies dominated by small and rounded opaque phytoclasts (Runcu Formation, P167R).

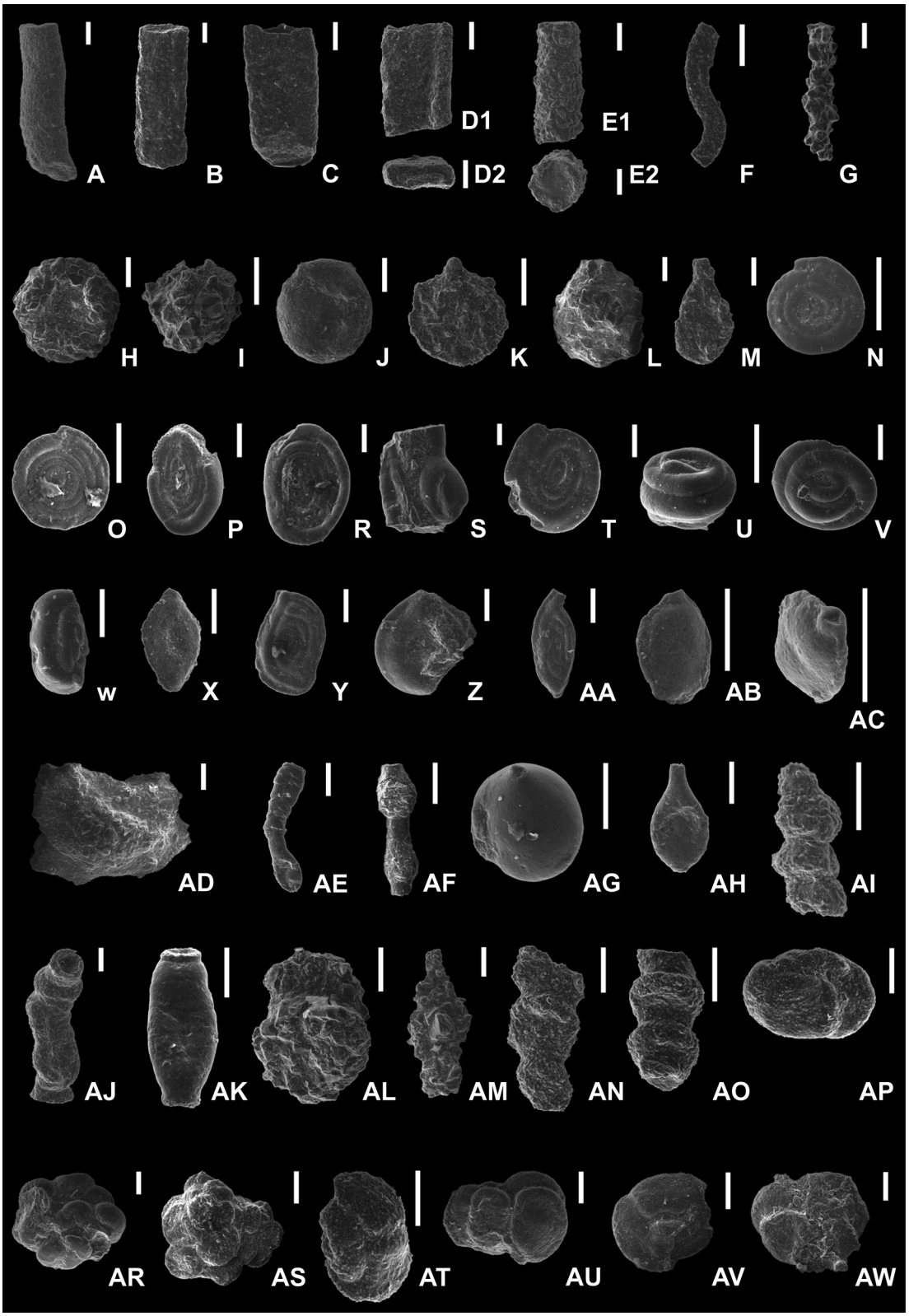

Fig. 6. Foraminiferal assemblages from the Varniţa section (scale bar: 200 μm). A. *Bathysiphon* sp., sample P155H. B. *Nothia excelsa*, P154H. C. *Nothia latissima*, P156H. D1-2. *Nothia robusta*, P167R. E1-2. *Psammosiphonella cylindrica*, P163R. F. *Rhizammina indivisa*, P155H. G. *Hyperammina rugosa*, P155H. H. *Psammosphaera irregularis*, P156H. I. *Psammosphaera fusca*, P165R. J. *Placentammina placenta*, P161H. K. *Saccammina grzybowskii*, P155H. L. *Saccammina sphaerica*, P164R. M. *Proteonina* sp., P169I. N. *Ammodiscus cretaceous*, P158H. O. *Ammodiscus tenuissimus*, P159H. P. *Ammodiscus peruvianus*, P159H. R. *Ammodiscus siliceous*, P167R. S. *Ammolagena clavata*, P163R. T. *Annectina grzybowskii*, P158H. U. *Glomospira charoides*, P160H. V. *Glomospira diffundens*, P156H. W. *Glomospira serpens*, P156H. X. *Rzehakina epigona*, P151H. Y. *Rzehakina fissistomata*, P169R. Z. *Rzehakina lata*, P165R. *AA. Rzehakina minima*, P165R. AB–AC. *Rzehakina inclusa*, P161H. AD. *Aschemocella grandis*, P160H. AE. *Aschemocella* cf. *subnodosiformis*, P152H. AF. *Caudammina excels*, P156H. AG. *Caudammina ovula*, P156H. AH. *Caudammina ovuloides*, P163R. AI. *Subreophax scalaris*, P155H. AJ. *Subreophax pseudoscalaris*, P155H. AK. *Kalamopsis grzybowskii*, P152H. AL. *Reophax duplex*, P169I. AM. *Reophax subfusiformis*, P155H. AN. *Hormosina trinitatensis*, P155H. AO. *Hormosina velascoensis*, P154H. AP. *Paratrochamminoides contortus*, P152H. AR. *Paratrochamminoides deflexiformis*, P163R. AS. *Paratrochamminoides mitratus*, P156H. AT. *Paratrochamminoides olszewskii*, P155H. AU. *Conglophragmium irregularis*, P163R. AV. *Trochamminoides irregularis*, P155H. AW. *Trochamminoides subcoronatus*, P155H.

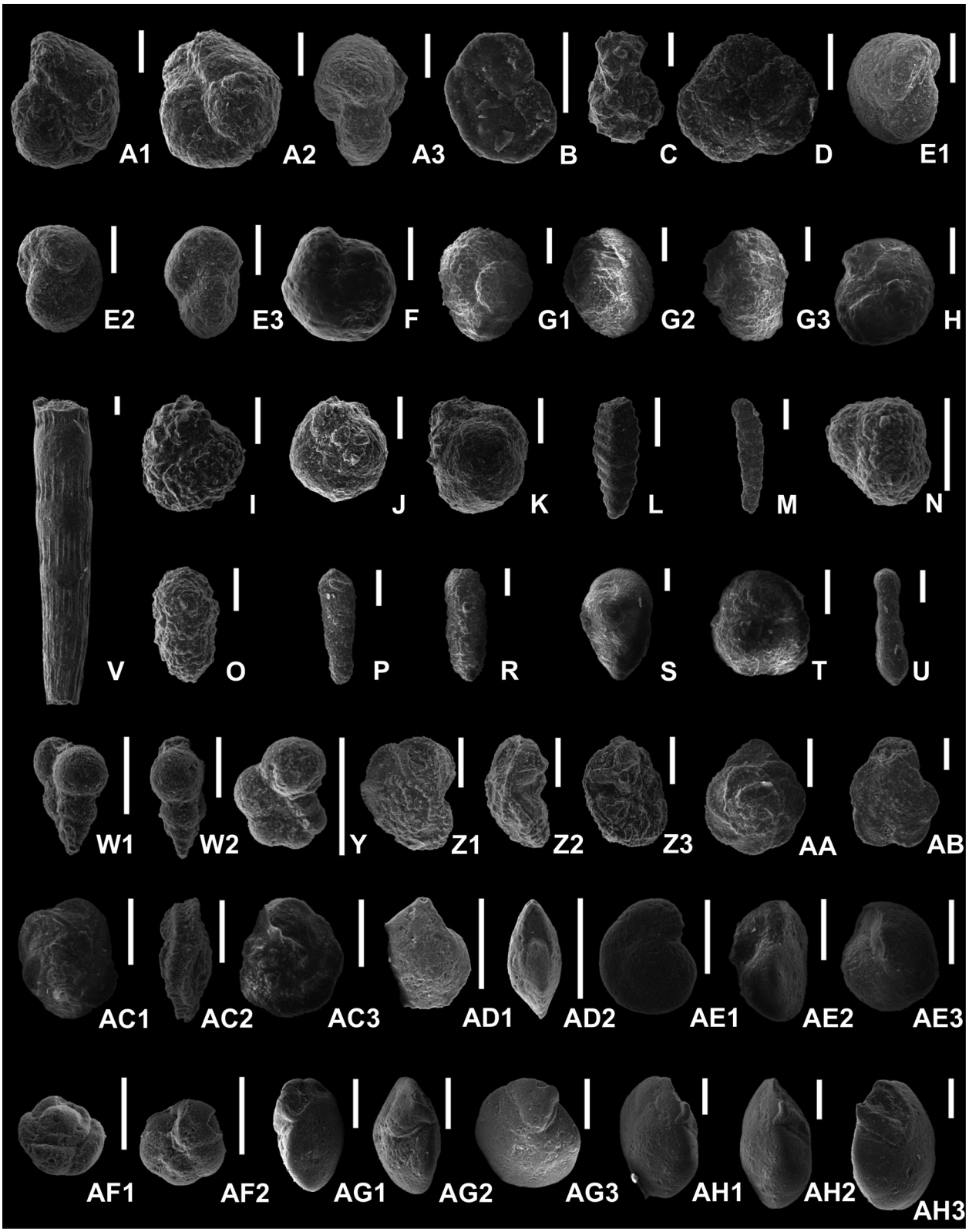

Fig. 7. Foraminiferal assemblages from the Varniţa section (scale bar: 200 μm). A1-3. *Haplophragmoides suborbicularis*, sample P155H. B. *Haplophragmoides walteri*, P155H. C. *Ammobaculites agglutinans*, P155H. D. *Ammosphaeroidina pseudopauciloculata*, P165H. E1-3. *Recurvoidella lamella*, P153H. F. *Recurvoides immane*, 168R. G1-3. *Recurvoides nucleosus*, P155H. H. *Recurvoides walteri*, P165R. I. *Thalmannammina recurvoidiformis*, P153H. J-K. *Thalmannammina subturbinata*, P168R. L. *Spiroplectammina spectabilis*, P152H. M. *Spiroplectammina navarroana*, P155H. N. *Conotrochammina whangaia*, P161H. O. *Karrerulina coniformis*, P155H. P. *Karrerulina conversa*, P160H. R. *Karrerulina horrida*, P155H. S. *Remesella varians*, P155H. T. *Eggerela trochoides*, P155H. U. *Dentalina* sp., P156H. V. *Dentalina megapolitana*, P152H. W1-2. *Heterohelix globulosa*, P158H. Y. *Hedbergella* sp., P151H. Z1-3. *Globotruncana arca*, P155H. AA. *Globotruncana stuartiformis*, P155H. AB. *Globotruncana schneegarsi*, P158H. AC1-3. *Abathomphalus mayaroensis*, P155H. AD1–2. *Lenticulina* sp., P158H. AE1-3. *Gyroidina girardanus*, P154H. AF1-2. *Gyroidinoides quadratus*, P155H. AG1-3. *Oridorsalis umbonatus*, P155H. AH1-3. *Eponides lotus*, P155H.

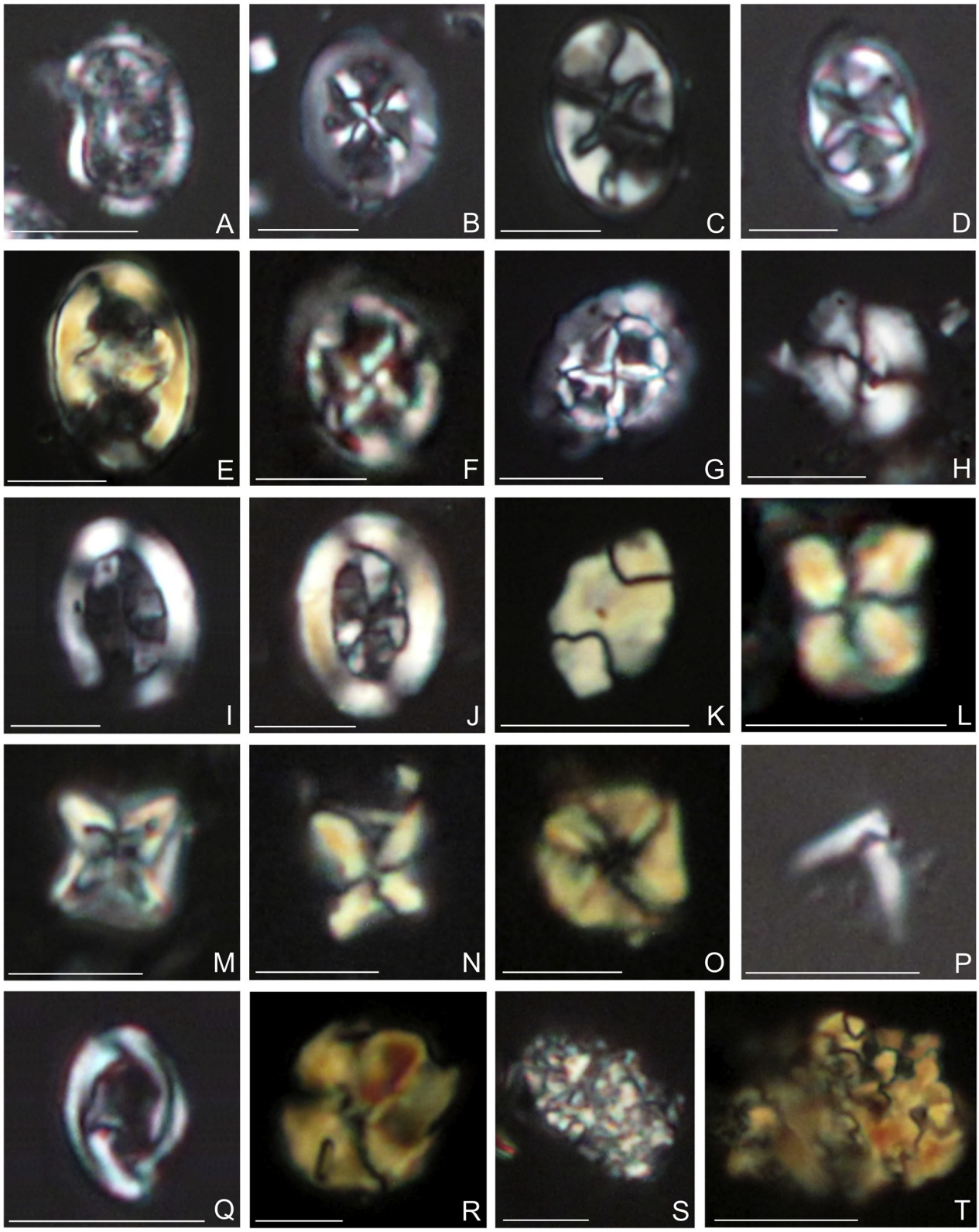

Fig. 8. Microphotographs of the late Maastrichtian-Danian calcareous nannofossil taxa from the Varniţa section (scale bar: 5 μm). A. *Nephrolithus frequens*, sample P152H. B. *Staurolithites mielnicensis*, P152H. C. *Eiffellithus turriseiffelii*, P160H. D. *Tegumentum stradneri*, P152H. E. *Zeugrhabdotus embergeri*, P159H. F. *Prediscosphaera cretacea*, P155H. G. *Prediscosphaera grandis*, P155H. H. *Watznaueria barnesiae*, P154H. I. *Arkhangelskiella cymbiformis*, P155H. J. *Arkhangelskiella maastrichtiensis*, P155H. K. *Calculites obscurus*, P157H. L. *Quadrum bengalensis*, P155H. M. *Micula staurophora*, P158H. N. *Micula* cf. *prinsii*, P161H. O. *Micula* cf. *praemurus*, P157H. P. *Ceratolithoides kamptneri*, P160H. Q. *Placozygus fibuliformis*, P155H. R. *Biantolithus sparsus*, P163R. S. *Thoracosphaera* sp., fragment, P163R. T. *Thoracosphaera* sp. fragment, P165R.

5. Results

5.1. Palynological content

Most samples yielded moderately rich palynological assemblages, consisting mainly of dinoflagellate cysts (32–93% of the total palynomorphs), spores and pollen grains (6–67%) and some foraminiferal linings, acritarchs and bryophytes. A total of 88 dinocyst species and subspecies were recorded in the studied succession (Appendix A). Among these marine palynomorphs, 35 taxa occur only in Maastrichtian deposits (Hangu Formation), 31 taxa in the Danian (Runcu and Izvor formations), while 22 species recorded from the Upper Cretaceous cross the K–Pg boundary and persist into the Danian. Generally, the continental palynomorphs have a higher frequency in the Maastrichtian strata; they consist of 13 pteridophyte genera, 18 taxa of angiosperms and gymnosperms, and two species of bryophytes (Appendix A).

In the Hangu Formation, 57 dinoflagellate species and subspecies were recognized. Among the taxa restricted to the Maastrichtian, the most abundant dinocyst species in some samples are *Chatangiella* sp. A of Schiøler and Wilson (1993) (with a peak abundance in P154H), *Cerodinium speciosum*, *Hystrichosphaeropsis quasicribrata*, *Hystrichosphaeridium tubiferum* and *Muratodinium fimbriatum*. However, most other dinocyst species recorded in the Hangu Formation are rare; these include *Chatangiella ditissima*?, *Leberidocysta chlamydata* subsp. *schiølerii*, *Membranilarnacia polycladiata*, *Palaeoperidinium pyrophorum* and *Thalassiphora pelagica* (Appendix A). The dinocyst taxa of which the LADs mark the top of the late Maastrichtian, such as *Diconodinium wilsonii*, *Dinogymnium cretaceum*, *Palynodinium grallator* and *Pterodinium cretaceum* have their last occurrence in the top of the Hangu Formation (samples P161H, P162H; Fig. 9).

Cerodinium diebelii, *Disphaerogena carposphaeropsis*, *Elytrocysta druggii*, *Hystrichosphaeridium tubiferum*, *Oligosphaeridium complex*, *Pterodinium cingulatum* and *Spiniferites* group were identified both in the Maastrichtian and Danian deposits. Generally, these taxa are more abundant in the Maastrichtian than in the Danian.

In the Danian strata (Runcu and Izvor formations), 53 dinocyst species were encountered. The most common taxa are *Spiniferites* and *Xenicodinium*, while *Achomosphaera ramulifera*, *A. regiensis*, *Cribroperidinium pyrum*, *Fibradinium annetorpense*, *Yolkinigymnium lanceolatum* have low abundances. In ascending order, species of which the FADs were considered previously as important markers for the early Danian, first occur in the Runcu Formation in P164R (*Kallosphaeridium yorubaense*, *Xenicodinium delicatum*, *X. lubricum*), and in sample P168R (*Tectatodinium pellitum*, *Xenicodinium reticulatum)*, and in the Izvor Formation in sample P169I (*Duosphaeridium rugosum*, *Hafniasphaera graciosa*, *Impagidinium maghribensis*, *Senoniasphaera inornata*, *Ynezidinium pentahedrias*) and in P170I (*Damassadinium californicum*). In the Runcu Formation, we have not recorded reworked palynological markers that would support the early-late Cretaceous age of debris flow deposits derived from the Audia and Hangu formations (Ionesi, 1997). The dinocyst species diversity encountered in the Izvor Formation is higher than in the Runcu Formation.

Terrestrial palynomorphs (fern spores, gymnosperms and angiosperms pollen) were frequently observed, mainly in the Hangu Formation. This spore-pollen assemblage occasionally shows frequencies up to 67% (sample P151H, Hangu Formation) of the total number of identified taxa, indicating a significant continental influence. Among the pteridophytes, *Deltoidospora*, *Leiotriletes* and *Polypodiaceoisporites* represent the most abundant taxa. Gymnosperm pollen grains include *Alisporites*, *Classopollis*, *Eucomiidites*, *Pinuspollenites*. The most frequent angiosperms are assigned to the Normapolles group. Tropical to subtropical conditions near the sedimentary basin can be inferred from the presence of *Cycadopites*, *Deltoidospora* and *Sapotaceoipollenites*.

In comparison with the Hangu Formation, a decrease in terrestrial palynomorphs was recorded during the sedimentation of the Runcu Formation, followed by a moderate diversification observed in the lower part of the Izvor Formation.

5.2. Foraminiferal assemblages

The microfossil assemblages in the Varniţa section contain a high number of agglutinated, calcareous planktonic and benthic foraminifera. One hundred and eleven taxa, represented by 1889 specimens (Appendix B), have been identified. The identified agglutinated assemblages are of the “flysch type” fauna, already known from the Cretaceous and Cenozoic bathyal turbiditic environments (Gradstein and Berggren, 1981; Kuhnt et al., 1989; Kaminski and Gradstein, 2005). The following 14 agglutinated foraminifera have a relative abundance exceeding 2% of the total identified specimens: *Ammodiscus* sp. (4.7%), *Bathysiphon* sp. (2.9%), *Caudammina excelsa* (4.5%), *Caudammina ovula* (4.5%), *Hormosina velascoensis* (2.27%), *Hyperammina rugosa* (2.5%), *Kalamopsis grzybowskii* (2.7%), *Nothia excelsa* (11.71%), *Paratrochamminoides* sp. (5.9%), *Placentammina placenta* (4.13%), *Psammosiphonela cilyndrica* (3.92%), *Recurvoides* sp. (4.4%), *Rhizammina indivisa* (2.22%) and *Saccammina grzybowskii* (3.18%). The benthic calcareous assemblage is characterized by representative taxa such as *Gyroidina* sp. (3.23%), *Gyroidinoides* sp. (1%), *Gyroidinoides quadratus* (1.2%) and *Pullenia jarvia* (2.12%). The most common planktic foraminifera are *Heterohelix* (2.5%) and *Globotruncana* (2.22%).

In the Hangu Formation, the Maastrichtian assemblages are dominated by agglutinated foraminifera (69 taxa), calcareous foraminifera being rare (11 planktic and 16 benthic taxa). The number of specimens varies between one (sample P162H) and 385 (sample P155H), and 59 taxa appear only in this formation. The planktonic foraminiferal assemblage (8.5%) consists of small unkeeled forms, such as *Globigerinelloides*, *Heterohelix* and keeled species of the *Abathomphalus* and *Globotruncana*. Planktonic foraminiferal specimens (e.g. *Heterohelix*) are more abundant (>50%) in the P151H and P157H samples. Relatively high numbers of specimens and a high diversity mark the Hangu Formation interval. The calcareous benthic foraminiferal assambleges (11%) consist of forms such as *Gyroidina*, *Gyroidinoides*, *Oridorsalis* and *Pullenia*. The foraminiferal assemblages from the Hangu Formation are highly diversified, compared to the assemblages identified in the Danian deposits.

In the Runcu and Izvor formations, agglutinated foraminifera dominate the assemblages, but several specimens of calcareous benthic foraminifera are also present, whereas calcareous planktonic foraminifera are absent.

In the Runcu Formation, 46 taxa of foraminifers have been identified (42 agglutinated foraminifera and 4 calcareous benthic foraminifera). The most abundant agglutinated foraminifera in this interval are *Ammodiscus* sp. (4.3%), *Bathysiphon* sp. (6.3%), *Caudammina ovula* (11.5%), *Hormosina velascoensis* (6.7%), *Kalamopsis grzybowskii* (3.4%), *Nothia excelsa* (17.2%), *Nothia robusta* (2.7%), *Paratrochamminoides* sp. (7.2%), *Psammosiphonella cylindrica* (12.5%), *Recurvoides* sp. (2%) and *Saccammina grzybowskii* (3.9%). The calcareous benthic foraminifera (2%) are represented by *Gyroidina*, *Gyroidinoides* and *Pullenia*.

The assemblage from the Izvor Formation includes 20 taxa, among which 16 are agglutinated and 4 are calcareous benthic foraminifera (e.g., *Gyroidina* sp. – 16.5%; *Pullenia jarvia* – 4.5%). Only two species were identified in the P170I sample: *Ammodiscus peruvianus* and *Caudammina ovula*. Moreover, the most abundant taxa in the formation are *Ammodiscus* sp. (9.1%), *Ammodiscus*

Fig. 9. Stratigraphic distribution of selected microfossils and bioevents in the Varniţa section. Planktonic foraminiferal zonation after Ogg et al. (2012) and agglutinated foraminiferal zones according to Olszewska (1997); calcareous nannofossil zonation: CC zones (after Sissingh, 1977; Perch-Nielsen, 1985), UC scheme (Burnett, 1998) and NP zones (Martini, 1971); dinocyst zones after Slimani (2001). Abbreviations: *P. hariaensis* = *Pseudoguembelina hariaensis*; *Pl. hantk.* = *Plummerita hantkeninoides*; *D. gal.* = *Deflandrea galeata*; *H. con.* = *Hystrichostrogylon coninckii*; *C.c* = *Carpatella cornuta.*

peruvianus (3.6%), *Hyperammina rugosa* (5.5%), *Nothia excelsa* (4.5%), *Psammosphaera* sp. (15.5%), *Recurvoides* sp. (4.5%) and *Rhizammina indivisa* (18.3%). The foraminiferal assemblage from the Izvor Formation has the lowest diversity compared to that of the Hangu and Runcu formations.

5.3. Calcareous nannofossils

The nannoplankton in the studied samples is characterized by variable diversity, abundance and preservation. We identified 48 taxa of the group (Appendix C), and an associated calcareous dinoflagellate genus *Thoracosphaera*. Generally, species richness varies between 8 and 14 taxa in the Hangu Formation, the highest species richness (20 taxa) being recorded in the P155H sample. The Runcu Formation contains four species and some of the samples from this formation, as well as from the Izvor Formation are barren. The preservation of calcareous nannofossils is poor to moderate throughout the studied section, due to carbonate dissolution on the sea bottom.

Overall, 44 taxa of calcareous nannofossils identified were restricted to the Hangu Formation. High frequencies of *Arkhangelskiella maastrichtiensis*, *Lucianorhabdus maleformis*, *Micula staurophora* and *Watznaueria barnesiae* (Appendix C) were found, while *Ceratolithoides kamptneri*, *Micula murus*, *Nephrolithus frequens*, *Quadrum bengalensis* and *Staurolithites minutus* have low frequencies.

Thoracosphaera sp. is the sole taxon identified both in the upper Maastrichtian and Danian deposits (Fig. 9). It is not very frequent in the upper Maastrichtian, but a bloom of the taxon (over 60%) was observed in the sample P163R (lower Danian of the Runcu Formation). The Runcu Formation also contains *Biantolithus sparsus*, *Cruciplacolithus* cf. *primus* and *Neocrepidolithus* cf. *fossus*.

5.4. Palynofacies compositions

In the studied section, the particulate organic matter (POM) is almost all of continental origin. Four main constituents of POM were recognized, namely: opaque phytoclasts, translucent phytoclasts, AOM (granular or gelified forms) and palynomorphs.

In the Hangu Formation the palynofacies is characterized by a moderate proportion of translucent phytoclasts (up to 44% in sample P154) and opaque phytoclasts (50–98%; Fig. 10) that are derived primarily from the oxidation of translucent material, which was transported over a prolonged period of time. Translucent organic particles are plant-derived fragments, in the Hangu Formation being mainly woody tissues, cuticles and numerous small fragments yellow-brown (in the web version) in color (Fig. 5P). The group is best represented in samples P154H, P161H and P162H (40–44%; Fig. 10). Opaque phytoclasts are occasionally frequent (samples P153H, P156H, P160H), being commonly small in size (10–40 μm) and rounded, more rarely lath-shaped. AOM shows a low frequency (up to 7% of total POM), the gelified type being predominant. The palynomorphs are pale yellow (in the web version) to pale brown (in the web version) and show low frequencies (0.5–2%) and values for C/M ratio ranging between −0.77 and 0.33 (Fig. 10). Occasionally, pollen grains and some woody tissues show framboidal pyrite on their surface (Fig. 5M), indicating an anoxic environment within the sediments. The palynofacies from the Hangu Formation also includes small amounts of foraminifer test linings.

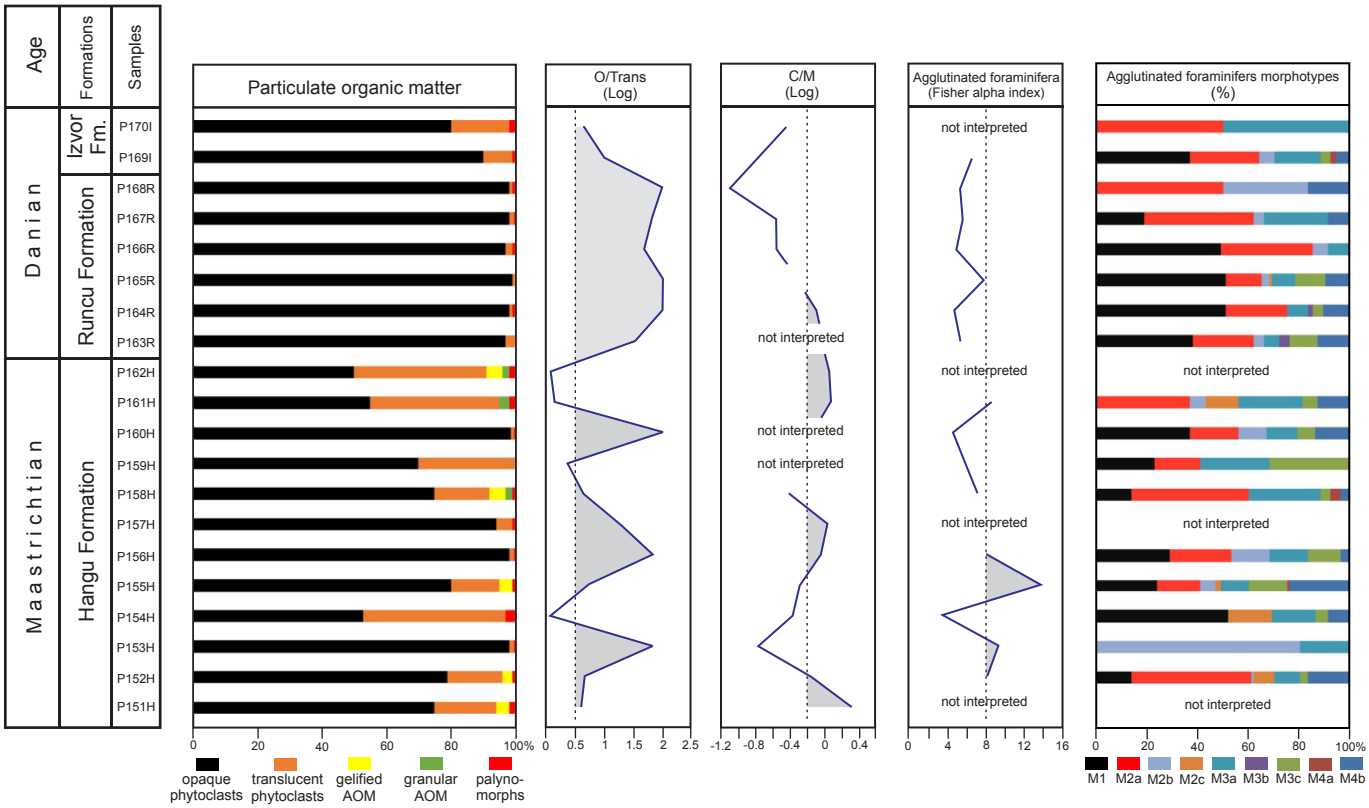

Fig. 10. Relative abundances of particulate organic matter and agglutinated foraminifers morphotypes in the Varniţa section. The palynofacies parameters (O/Trans, C/M) distribution and Fisher alpha diversity index are also shown. O/Trans = opaque to translucent phytoclasts ratio; C/M = continental/marine palynomorphs ratio.

In the Runcu Formation, a decrease in the POM amount was observed, compared to that in the Hangu Formation. Furthermore, the organic matter is characterized by a high opaque phytoclasts proportion (97–99%) and these clasts usually have a small size (10–30 μm) and a rounded shape (Fig. 5Q). Such "allochthonous" fractions of organic particles are refractory to any further biochemical oxidation and can be distributed far from their terrestrial source area in marine basins. However, a limited amount of this organic matter could have been reworked from older Cretaceous deposits, since the Runcu Formation consists of debris-flow deposits (Ionesi, 1997). The translucent particles show low frequencies (1–3%), the palynomorphs are poorly preserved, sometimes being absent (samples P163R and P165R).

In the lower part of the Izvor Formation (samples P169I and P170I), a slight increase in the POM amounts was observed. The palynofacies is dominated by opaque phytoclasts (P169I, 90% of total POM), followed by an increase in translucent particles content in sample P170I (18%; Fig. 10). The mean size of the phytoclasts varies markedly, from mostly 10–15 μm to 90 μm. The P170I sample contains many palynomorphs with a good preservation, dinocysts being predominant (74% of total palynomorphs).

6. Discussion

6.1. Biostratigraphy

The dinoflagellate cysts, foraminifera and calcareous nannoplankton assemblages were used to establish of a biostratigraphic framework for the 52 m thick section of the Varniţa outcrop. The age determinations are based on the FADs and the LADs of significant marker taxa.

6.1.1. Late Maastrichtian

The first nannoplankton bioevent recorded in the lowermost part of the studied section (Hangu Formation) is the first occurrence (FO) of *Nephrolithus frequens* in sample P152H (Fig. 9). This datum is widely used as a biostratigraphic marker for the late Maastrichtian, indicating the subzones CC26a (Sissingh, 1977) and UC20c^{TP} (Burnett, 1998). In the Romanian Carpathians, the taxon was recorded in the Gura Beliei Formation (the uppermost 15 m at the top of the Maastrichtian; Bojar et al., 2009), as well as from the upper part of the Hangu Formation (Bojar and Bojar, 2013). The next bioevent observed toward the top of the Hangu Formation is the occurrence of *Micula* cf. *prinsii*, which is restricted to the sampling interval P158H–P161H. This nannofossil event defines the uppermost part of the Maastrichtian, more precisely the CC26b and UC20d^{TP} subzones (Sissingh, 1977; Burnett, 1998). The nannofossil assemblages identified only in the P152H–P162H interval also contain *Arkhangelskiella cymbiformis*, *A. maastrichtiensis*, *Ceratolithoides kamptneri*, *Lithraphidites quadratus*, supporting a late Maastrichtian age for the interval.

The late Maastrichtian age for the deposits assigned to the Hangu Formation is also supported by several dinocyst events, namely: the FOs of *Cerodinium speciosum*, *Deflandrea galeata*, *Disphaerogena carposphaeropsis*, *Turbiosphaera filosa* and the last occurrences (LOs) of *Chatangiella* sp. A of Schiøler and Wilson (1993), *Dinogymnium* spp., *Isabelidinium cooksoniae*, *Palynodinium grallator* and *Pterodinium cretaceum*. The FAD of *Deflandrea galeata* and LADs of *Chatangiella* sp. A Schiøler and Wilson (1993) and *Isabelidinium cooksoniae* occur in the late Maastrichtian in many areas of the Northern Hemisphere (Schiøler and Wilson, 1993; Slimani, 2000, 2001; Slimani et al., 2010, 2011, 2016; Guédé et al., 2014). In the Varniţa section, the FO of *Deflandrea galeata* and the LO of *Chatangiella* sp. A and *Isabelidinium cooksoniae* are observed in samples P151H and P155H, respectively (Fig. 9). In the lower part of the section (P151H and P152H), two marker taxa (*Chatangiella ditissima*? and *Alterbidinium* sp. cf. *A. varium*) which have their LADs in the lower Maastrichtian were identified, but undoubtedly these finds are reworked specimens from older deposits. *Cerodinium speciosum* has its FAD in the middle part of the upper Maastrichtian (*Deflandrea galeata* zone) from Belgium, according to Slimani (2001). Moreover, several authors (e.g., Slimani and Toufiq, 2013; Mohamed et al., 2013; M'Hamdi et al., 2015; Slimani et al., 2016) record the taxon in the upper Maastrichtian–Paleocene deposits. In our section, the species first occurs in sample P154H. *Disphaerogena carposphaeropsis* is another taxon which supports the late Maastrichtian age for the top of the Hangu Formation. The FAD of this species was frequently recorded in the uppermost Maastrichtian of the Northern Hemisphere (Slimani et al., 2010, 2016; M'Hamdi et al., 2013; Mohamed et al., 2013; Guédé et al., 2014). In the studied section, the taxon could be followed from sample P158H (Hangu Formation) to sample P168R (Runcu Formation).

Other dinocyst events defining the latest Maastrichtian are the LADs of *Dinogymnium cretaceum*, *Palynodinium grallator* and *Pterodinium cretaceum* in the Boreal and northern Tethyan realms (Hansen, 1977; Schiøler and Wilson, 1993; Habib et al., 1996; Slimani, 2001; Williams et al., 2004; Slimani et al., 2011, 2016). These taxa have their last occurrences in samples P161H and P162H (top of the Hangu Formation), confirming the late Maastrichtian age for the interval given above. According to Slimani (2001), his uppermost Maastrichtian *Hystrichostrogylon coninckii* Zone, which is correlated with the *Palynodinium grallator* Zone of Hansen (1977), is subdivided into two successive subzones "a" and "b". The base of the Subzone "a" lies between the LO of *Isabelidinium cooksoniae* and the FO of *H. coninckii*, and its top is marked by the LO of *Diconodinium wilsonii*. The subzone "b" is confined between the LO of the *D. wilsonii* and the FO of the Danian marker *Damassadinium californicum*. In our section, the occurrence of *D. wilsonii* only in sample P162H (top of the Hangu Formation) would indicate the absence of a stratigraphic interval (subzone "b" of the *H. coninckii* Zone; uppermost Maastrichtian) in the studied lithological column. However, in our opinion, subzone "b" of the *H. coninckii* Zone might be confined to the approximately 16 m thick interval (P162H to P163R; Fig. 9) which is covered by the landslide. The absence of this interval is supported by the absence from the assemblage of the dinoflagellate cyst *Manumiella seelandica* (senior synonym of the *Manumiella druggii*; Yepes, 2001), the FO of this taxon indicating the latest Maastrichtian in the Northern Hemisphere (Brinkhuis and Zachariasse, 1988; Williams et al., 2004; Slimani et al., 2010, 2016; M'Hamdi et al., 2013; Guédé et al., 2014; Vellekoop et al., 2015).

The dinoflagellate cysts *Deflandrea galeata*, *Palynodinium grallator* and *Pterodinium cretaceum*, were identified in the Eastern Carpathians from the uppermost 15 m thick interval assigned to the Lepşa Formation (Runcu section, Vrancea Nappe) by Ţabără and Slimani (2017). This dinocyst assemblage allows a correlation of the interval from the Lepşa Formation with the upper part of the Hangu Formation studied here.

The foraminiferal assemblages of the Hangu Formation contain some marker taxa frequently used for the upper Maastrichtian biozonation. The *Abathomphalus mayaroensis* Zone is the stratigraphic interval represented by the total range of the nominate index species, indicating the upper Maastrichtian in many sections from the Tethyan realm (Ionesi and Tocorjescu, 1968; Caron, 1985; Tshakreen and Gasiński, 2004; Gasiński and Uchman, 2009; Gasiński et al., 2013; Kędzierski et al., 2015). In our section, *A. mayaroensis* occurs in the Hangu Formation in samples P155H and P158H (Fig. 9).

The late Maastrichtian age is also supported by the agglutinated foraminifera *Remesella varians* and *Rzehakina inclusa*, which define

the *R. inclusa* Zone according to Olszewska (1997). Both taxa occur in the Hangu Formation in the P155H–P161H interval (Fig. 9; Appendix B). *Remesella varians* ranges from the late Maastrichtian to the Paleocene (Kaminski and Gradstein, 2005; Oszczypko et al., 2005) and it also occurs in the Runcu Formation (sample P169I).

Summing up, all the bioevents distinguished above, revealed by dinocysts, nannoplankton and foraminifera marker taxa, support the late Maastrichtian age for the upper part of the Hangu Formation (interval P151H–P162H).

6.1.2. Danian

Above the K–Pg boundary in the Romanian Carpathians (the lowermost 4–5 m thick interval of the lower Danian), Melinte and Jipa (2005) and Bojar et al. (2009) reported two successive blooms of the calcareous dinoflagellate genus *Thoracosphaera* and of the nannofossil species *Braarudosphaera bigelowii* in the Pietroşiţa section. The blooms have been also recorded slightly above the K–Pg boundary event in many other areas (Smit and Romein, 1985; Pospichal, 1996; Lamolda et al., 2005). A bloom, but only of the *Thoracosphaera*, has been identified by us in the samples P163R (60–70%) and P164R (Runcu Formation), suggesting an early Danian age for the interval. However, from the Varniţa section, Bojar and Bojar (2013) report in the lowermost Danian (upper part of the Hangu Formation), a bloom of the *Thoracosphaera* and a drop in frequency for the *Micula* spp. and *Watznaueria barnesiae*. These events are not in agreement with our results obtained for the Hangu Formation, according to which *Thoracosphaera* shows a low frequency in almost all samples, from P151H to P162H. In addition to the bloom of the *Thoracosphaera* (recorded in P163R and P164R), we identified in the same samples nannoplankton taxa *Biantolithus sparsus* (NP1–NP10 zones), *Cruciplacolithus* cf. *primus* (NP1–NP9 zones) and *Neocrepidolithus* cf. *fossus* (NP1–NP4 zones), indicating a Paleocene age.

All the biostratigraphic data based on nannoplankton from the Runcu Formation discussed above, differ slightly compared to other interpretations (e.g., Ionesi, 1997), which assign a late Danian age (NP4 Zone, based on *Ellipsolithus macellus*) for the formation.

The dinoflagellate cysts confirm the early Danian age, inferred based on the nannoplankton in sample P164R, by the FOs of *Kallosphaeridium yorubaense*, *Xenicodinium lubricum* and *X. reticulatum*. The dinocysts *Xenicodinium lubricum* and *X. reticulatum* have well-documented FADs in the lower Danian (Hansen, 1977; Powell, 1992; Hardenbol et al., 1998; Slimani, 2000, 2001; Vasilyeva and Musatov, 2012). The stratigraphic range of these dinocyst taxa in the studied section can be correlated with the *Xenicodinium lubricum* Zonule (upper part of the *Damassadinium californicum* Zone; Hansen, 1977) established in the Danian limestones from Denmark. In the Eastern Carpathians, the *Xenicodinium lubricum* was also recorded in the lower Danian deposits of the lower part of the Putna-Piatra Uscată Formation (Ţabără and Slimani, 2017). *Carpatella cornuta*, the zonal species of the lowermost Danian *Carpatella cornuta* Zonule (lower part of the *Damassadinium californicum* Zone; Hansen, 1977) is not recorded in our section. The absence of the species might be related to either its extreme scarcity or the unfavorable environmental conditions.

The lower Danian is also characterized by the FADs of *Kallosphaeridium yorubaense*, *Tectatodinium pellitum* and *Xenicodinium delicatum* (Hansen, 1977; Slimani, 1995, 2001; Slimani et al., 2010; M'Hamdi et al., 2013). Their occurrence (P164R–P168R; Fig. 9) in the studied section supports the Danian age of the analyzed interval in the Runcu Formation.

The *Rzehakina fissistomata* Zone, defined by the first and last occurrence of the species, is characteristic for the Paleocene of the Carpathians Mountains (Ionesi and Tocorjescu, 1968; Olszewska, 1997; Bąk and Wolska, 2005; Bindiu and Filipescu, 2011; Cieszkowski et al., 2012). Recently, Kędzierski et al. (2015) record the first occurrence of the *Rzehakina fissistomata* in the uppermost Maastrichtian of the Polish Carpathians. In the studied section, this taxon was recorded starting with the sample P165R (Fig. 9), slightly above the first occurrence of the *Xenicodinium lubricum*, which is a dinocyst marker for the early Danian.

The two samples P169I and P170I analyzed from the lower part of the Izvor Formation contain global Danian index dinocysts such as *Damassadinium californicum* and *Senoniasphaera inornata*, valuable for the identification of the K–Pg boundary in many areas (Brinkhuis and Zachariasse, 1988; Gedl, 2004; Williams et al., 2004; Prauss, 2009; Slimani et al., 2010, 2016; Willumsen, 2011; Slimani and Toufiq, 2013; Dastas et al., 2014; Guédé et al., 2014). The stratigraphic range (FAD and LAD) of *Senoniasphaera inornata* is restricted to the lower-middle Danian interval (66–62.6 Ma; Hardenbol et al., 1998; Williams et al., 2004; Slimani et al., 2010; Gradstein et al., 2012). The occurrence of the species in samples P169I and P170I suggests that the lower part of the Izvor Formation is not younger than the middle Danian. The FAD of *Damassadinium californicum* marks globally the lowermost Danian at 65.8 Ma, while its LAD is placed at 60.33 Ma (lowermost Selandian) in the Northern Hemisphere middle latitudes (Hardenbol et al., 1998; Williams et al., 2004).

The dinoflagellate species *Duosphaeridium rugosum*, *Hafniasphaera graciosa*, *Impagidinium maghribensis*, *Tectatodinium pellitum* and *Ynezidinium pentahedrias*, which have well-documented FADs in the Danian (Hansen, 1977; Head, 1994; Slimani et al., 2008, 2010; Vasilyeva, 2013) were recorded only in the Izvor Formation, and therefore confirm the Danian age for this interval.

Our biostratigraphical attributions based on dinocysts do not support those presented by Antonescu and Alexandrescu (1979), which establish a Thanetian age for the Izvor Formation, based on *Cerodinium speciosum*, *Duosphaeridium rugosum* and *Trithyrodinium evittii*. The Thanetian age of the Izvor Formation is supported, according to the same authors by *Cerodinium speciosum*, considered as a marker taxon for this age. We found the species only in the Hangu Formation (Fig. 9), the FAD of the taxon dating from the late Maastrichtian, as previously mentioned.

Pentadinium darmirae sp. nov. is described below. It has been identified only in the Danian deposits of the Varniţa section, assigned to the Runcu Formation and lower part of the Izvor Formation (interval P164R–P170I; Fig. 9). The taxon was already recorded as *Pentadinium* sp. A in the lower part of the Putna-Piatra Uscată Formation (lower Danian) from the Eastern Carpathians by Ţabără and Slimani (2017).

In the lower part of the Izvor Formation, only agglutinated foraminifera occur. Among these, *Rzehakina fissistomata* supports the Danian age for this interval. Calcareous nannofossils were not found in the two samples analyzed from the Izvor Formation. The absence in the assemblage of the calcareous microfossils (foraminifera and nannoplankton) from this interval can be explained by calcite dissolution in marine deposits (Thierstein, 1980; Schiebel et al., 2007).

6.2. Palaeoenvironmental reconstruction

The sedimentary organic matter, also called kerogen, recorded from the strata discussed here includes a large proportion of continental material, with phytoclasts, pollen grains and spores, as well as a small amount of marine material composed of dinoflagellate cysts and granular AOM (Fig. 10). In the stratigraphic interval analyzed from the Varniţa section, all morphotypes of agglutinated foraminifers were also identified. M1 (tubular specimens, indicative for a bathyal environment; Jones and Charnock, 1985; Murray et al., 2011) and M2a (shallow infauna) morphogroups are

prevalent in almost all the samples, occasionally exceeding together 50% of the assemblages (Fig. 10).

The kerogen analyzed from the Hangu Formation samples is mainly composed of opaque phytoclasts (small in size and rounded shape) that are derived primarily from the oxidation of terrestrial plant tissue, as well as translucent phytoclasts (up to 44%). The O:Trans ratio in the Hangu Formation shows values of 0.08–1.9 (Fig. 10), suggesting some changes of the palaeoenvironment, from outer shelf to distal depositional environments. The same environments are also indicated by the C/M ratio, the latter having a higher value in samples P151H and P157H (Fig. 10), and a slightly lower value in sample P153H, due to the poorness representation of the terrestrial palynomorphs in the latter sample. The SPM ternary diagram of Federova (1977) also supports shallow marine to offshore marine depositional environments for the deposits assigned to the Hangu Formation (Fig. 11).

The Hangu Formation in our section also contains almost all morphogroups of agglutinated foraminifera, except for M3b. The occurrence of tubular forms (M1), as well as deep-water agglutinated foraminifera (e.g. *Paratrochamminoides*, *Psammosphaera*, *Saccammina*) indicate a bathyal environment for this stratigraphic interval.

The species diversity of the benthic foraminifera usually increases with water depth, as a result of the decreasing of organic carbon flux to the sea floor (Murray, 2006; pp. 250–254). In the Varniţa section, high species diversity was noted in the Hangu Formation (with Fisher alpha diversity index ranging from 3.4 to 13.7; Fig. 10), while the foraminiferal assemblages of the Runcu and Izvor formations show a slight decrease in diversity (Fisher alpha diversity index 4.6–7.7). Relatively high numbers of specimens and diversity are recorded in the P155H–P156H interval, and interpreted to reflect a distal depositional environment. In contrast, the number of specimens is low in the Runcu Formation (samples P166R to P168R), this interval mainly consisting from debris-flow deposits. The decrease of the diversity in the assemblages from the upper Maastrichtian to the Paleocene might also be related to the K–Pg event, although generally benthic foraminifera appear to be less affected by the global extinction event (Coccioni and Marsili, 2007; Kaminski et al., 2010; Machalski et al., 2016).

A few meters above the sample P155H (Fig. 2) in the Hangu Formation, many spheroidal aggregates of framboidal pyrite were identified (Fig. 12B,C). The size of the aggregates ranges from 30 (most often) to 80 μm and the concretions are composed of closely intergrown octahedral crystals. Pyritized organic remains are common in the sedimentary record and have been identified in the molds of diatoms (Schallreuter, 1984; McNeil, 1990), gastropods and bivalves (Fisher, 1986) or recent foraminifers (Seiglie, 1973). According to our observations, the spheroidal aggregates identified in the Hangu Formation are very similar to those described by Schallreuter (1984) from inside diatoms in the Angola Basin. Generally, the framboidal pyrite replaces the organic matrix or "soft parts" during all the stages of the sediment burial history, its formation requiring anoxic conditions within the sediments or inside of the microfossils (Canfield and Raiswell, 1991; Szczepanik et al., 2004). In our case, some anaerobic microenvironments formed inside of microfossils allowed the growth of bacteria (e.g., *Desulphovibrio desulphuricans*), which reduced sulphates from the surrounding sea water to sulphide. According to Szczepanik et al. (2004), formation of the framboids in the microfossils does not require a hosting anoxic environment. Framboidal pyrite also occurs in the Hangu Formation both as free octahedral crystals used

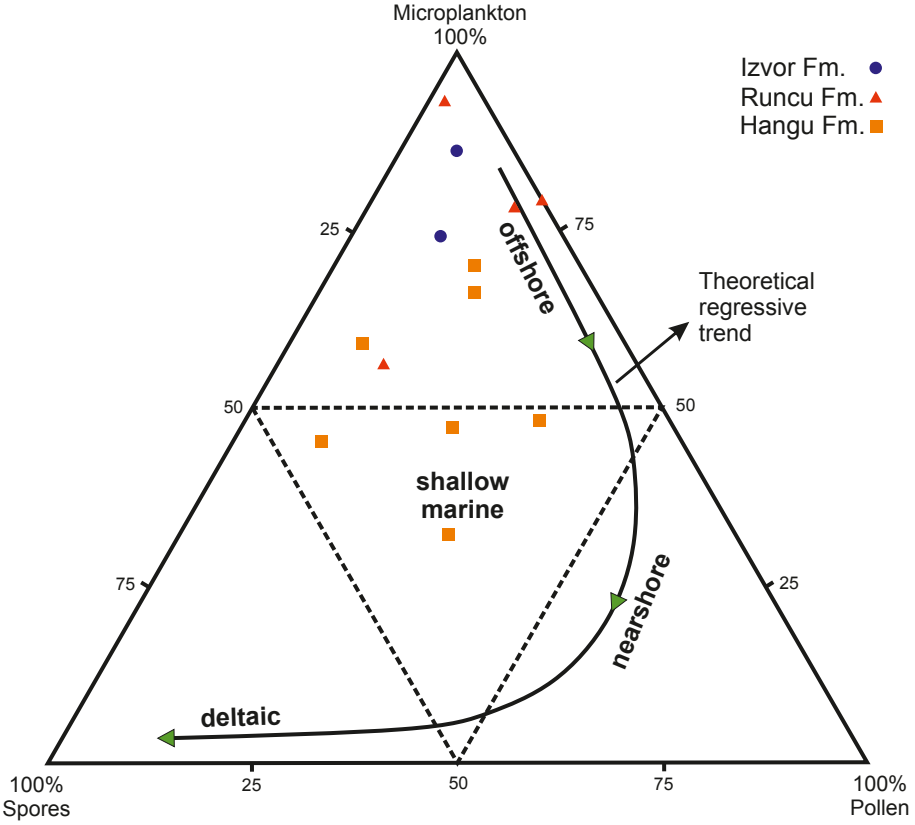

Fig. 11. Spore–pollen–microplankton ternary plot (after Federova, 1977; Duringer and Doubinger, 1985), with inferred depositional environments of the geological formations analyzed.

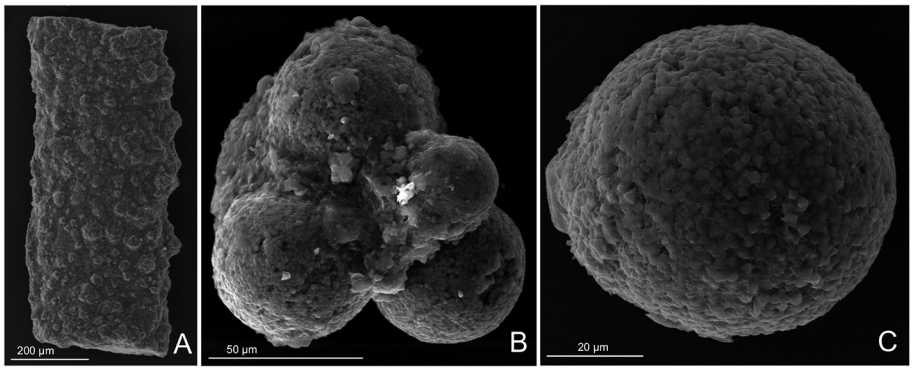

Fig. 12. SEM image of a framboidal pyrite identified in the Hangu Formation. A. Test of agglutinated foraminifer (*Nothia* sp.), consisting of many octahedral crystals and spheroidal aggregates of framboidal pyrite. B, C. Spheroidal aggregates of framboidal pyrite built mainly of octahedral crystals, probably crystallized inside diatoms due to sulfate-reducing bacteria.

by some agglutinated foraminifera to build their own tests (Fig. 12A), as well as on sporomorph exine (Fig. 5M).

The Runcu and the Izvor formations show modifications in the palynofacies composition (Fig. 10) due to some changes of the depositional environment, compared to that of the upper Maastrichtian. The kerogen analyzed from the Runcu Formation is composed mainly of opaque phytoclasts (97–99%), having small dimensions and rounded shapes as a result of prolonged transport. Thus, a transgressive trend during sedimentation of the Danian deposits is documented by increasing values of the O:Trans ratio (Fig. 10), the decrease of the C/M ratio, as well as by high frequency of the marine microplankton (Fig. 11).

In the Runcu Formation, all morphogroups of agglutinated foraminifera were identified. Morphotype M3b (*Ammolagena clavata*, samples P163R and P164R) which is used as an indicator of paleobathymetry (upper bathyal to abyssal, Kaminski and Gradstein, 2005) as well as high amounts of tubular forms (M1) which occur in the same assemblages with some "flysch-type" taxa (e.g. *Recurvoides*, *Thalmannammina*), suggest a bathyal environment, deeper than that of the upper Maastrichtian environment. This depositional environment is also suggested by the calcareous foraminifera and calcareous nannofossils distributions. The deposits assigned to the Runcu and Izvor formations are almost devoid of calcareous microfossils, which would indicate that their sedimentation took place near, but slightly above the Carbonate Compensation Depth (CCD). However, this inference should be carefully considered because both the nannoplankton and calcareous foraminifera suffered a decrease in the abundance at the end of the Cretaceous.

7. Systematic palynology

Division Dinoflagellata (Bütschli, 1885) Fensome et al., 1993
Subdivision Dinokaryota Fensome et al., 1993
Class Dinophyceae Pascher, 1914
Subclass Peridiniphycidae Fensome et al., 1993
Order Gonyaulacales Taylor, 1980
Suborder Gonyaulacineae (autonym)
Family Gonyaulacaceae Lindemann, 1928
Subfamily Gonyaulacoideae Autonym

Genus *Pentadinium* Gerlach, 1961, emend. Benedek et al., 1982
Type species: *Pentadinium laticinctum* Gerlach, 1961, emend. Benedek et al., 1982

Pentadinium darmirae Slimani and Ţabără sp. nov.
Fig. 13A–L

2017 *Pentadinium* sp. A, Ţabără and Slimani, Fig. 4(C), table 1.

Derivation of name. Named after the twin daughters (Daria and Miruna) of the second author (Daniel Ţabără) of the species.
Holotype. Sample P168R, slide 5, EF Z26/2 (Fig. 13A–C).
Paratype. Sample P168R, slide 3, EF A53/4 (Fig. 13E–G).
Repository. Botanical collection of the National Herbarium (RAB), Scientific Institute, University Mohammed V of Rabat, Morocco.
Type locality. Varniţa section, northern Eastern Carpathians.
Stratigraphic horizon. Runcu Formation and lower part of the Izvor Formation (lower– middle Danian).
Diagnosis. A species of *Pentadinium* with moderately thick and smooth to shagreenate endophragm and a thin, hyaline, delicate and smooth to shagreenate periphragm. Gonyaulacoid tabulation indicated by high sutural folds or cavate crests. The species is characterized by a distinct apical pericoel resulting from a complete endo-periphragm separation at the apical plates and by a large untabulated ventral area. Archeopyle formed by release of precingular plate 3″. Operculum free.
Description. Medium sized (55–90 µm), suturocavate, ovoidal to subspherical cyst with a thick (~2 µm) and smooth to shagreenate endophragm and a thinner (~0.5 µm), hyaline, delicate and smooth or rarely shagreenate periphragm. The periphragm is closely appressed to the endophragm at the central areas of the plates, but separated along the plate margins to form cavate sutural crests or folds, except for the apical area, where the two wall layers are completely separated at the apical plates to form a distinctive prominent pericoel. The tabulation is gonyaulacoid (4′? 3–6″, 3–6c, 3‴–6‴, 1p?, 1⁗) and incompletely developed in the ventral surface. It is reflected by 3 precingular (2″, 3″, 4″), 3 cingular (2c, 3c, 3c), 3 postcingular (2‴, 3‴, 4‴) and 1 antapical (1⁗) plates. The apical plates are not reflected due to the complete separation of the periphragm and endophragm. In the ventral surface, the sulcal and adjacent precingular and postcingular plates are not reflected by the periphragm and form a large untabulated ventral area, the endophragm and periphragm are closely appressed at this area and show no indication of tabulation. Archeopyle precingular type P (3″). Periarcheopyle larger than endoarcheopyle. Operculum pentagonal, free, detached or in place.
Dimensions (in µm). Holotype, paratype and range for 20 specimens measured: overall length 90, 73, 55(70)90; overall width 65, 60, 52(60)68; central body length 55, 55, 44(51)55; central body width 52, 50, 40(47)52.
Remarks. *Pentadinium darmirae* sp. nov. is unique in having smooth to shagreenate endo- and periphragm, a distinctive apical pericoel and a consistent large untabulated ventral area, where sulcal and adjacent precingular and postcingular plates are not reflected. *Pentadinium laticinctum* subsp. *laticinctum* resembles the new species by the smooth surface of the endocyst, but differs in having an

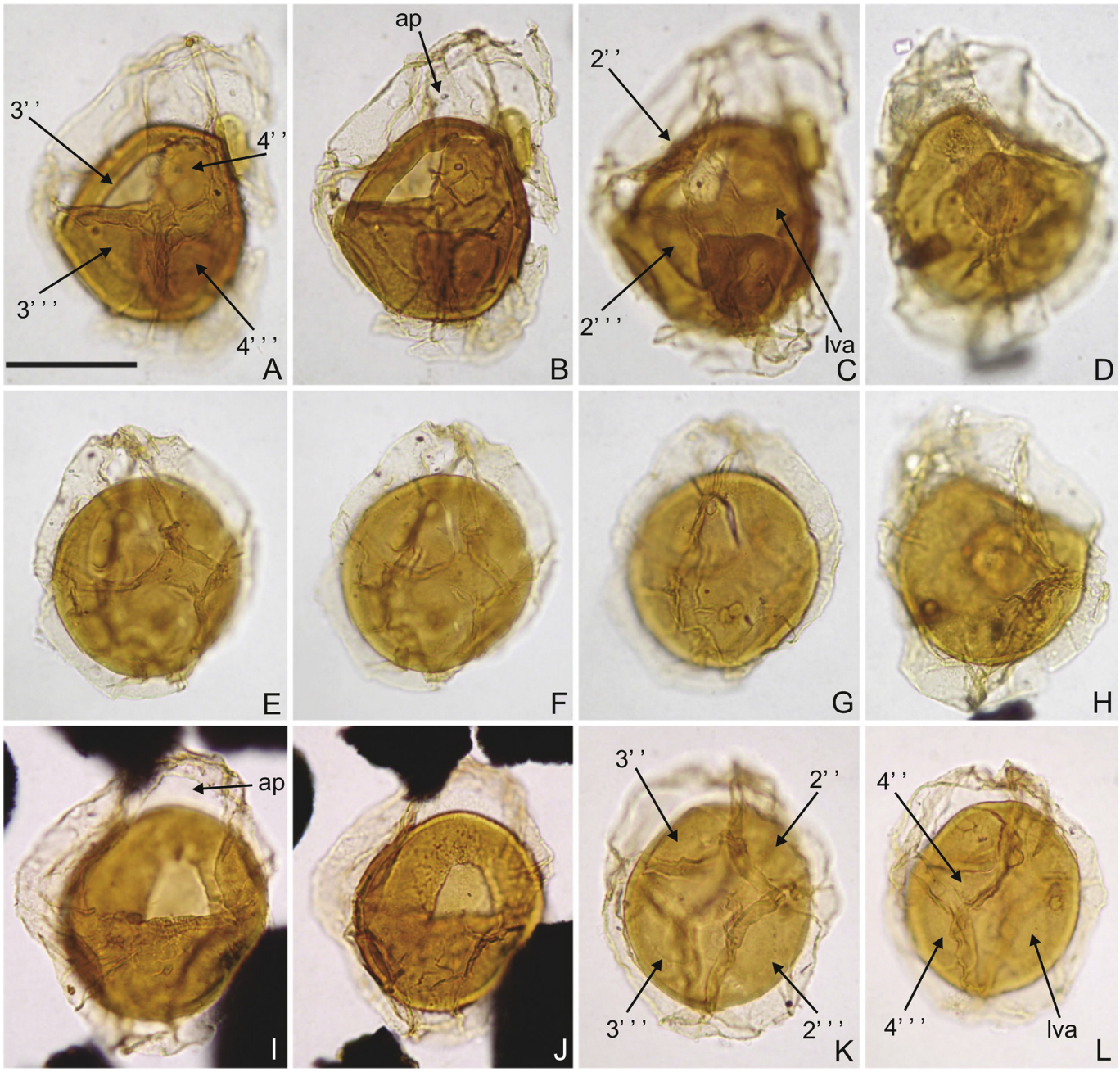

Fig. 13. *Pentadinium darmirae* Slimani and Ţabără sp. nov. from the Danian of the Varniţa section, northern Eastern Carpathians. Scale bar in A represents 30 μm for all specimens illustrated. A–C, holotype, left dorsolateral view, sample P168R, slide 5, England Finder reference Z26/2. A, left dorsolateral surface showing the precingular 4″ and postcingular 3‴, 4‴ plates and the precingular archeopyle; B, optical section; C, right ventrolateral surface showing the operculum, the precingular 2″ and postcingular 2‴ plates and a large ventral area (lva) without indication of tabulation. Note the prominent apical pericoel (ap), where the periphragm is completely detached from the endophragm. D, H, right dorsolateral view, sample P168R, slide 8, England Finder reference O55. D, right dorsolateral surface showing the precingular archeopyle and operculum; H, right ventrolateral surface with a large untabulated ventral area. E–G, paratype, ventral view, sample P168R, slide 3, England Finder reference A53/4. E, dorsal surface, low focus on the sutural crests and precingular archeopyle; F, focus on the dislocated operculum; G, high focus of the ventral surface showing a large untabulated area. I–J, ventral view, sample P168R, slide 11, England Finder reference X41. I, dorsal surface, low focus on the precingular endo- and periarcheopyle archeopyle, and on the cingulum; J, ventral surface with a high focus on the large untabulated area. K–L, left ventrolateral view, sample P168R, slide 6, England Finder reference E28. K, right dorsolateral surface, low focus on the precingular archeopyle and the precingular 2″ and postcingular 2‴, 3‴ plates, indicated by sutural folds; L, left ventrolateral surface showing the operculum in place, the precingular 4″ and postcingular 4‴ plates and a large untabulate area.

indication of apical and precingular and postcingular plates adjacent to the sulcus. Moreover, the new species present a consistent and prominent apical pericoel, where the periphragm is completely detached from the endophragm. *Pentadinium alabamensis* also has a smooth endocyst as in *Pentadinium darmirae* sp. nov., but differs especially by its perforate periphragm. Other species (*Pentadinium galileoi*, *Pentadinium polypodum*, *Pentadinium spinulum*) have a relatively smooth surface of the endocyst, but differ from the new species in possessing processes. The other species of the genus *Pentadinium* can be easily distinguished from the new species in having an ornamented rather than smooth surface of the endocyst. The endocyst surface structure of these species may be granular to vermiculate in *Pentadinium*? *circumsutum*, *Pentadinium corium*, *Pentadinium goniferum*, *Pentadinium imaginatum*, *Pentadinium laticinctum* subsp. *granulatum*, *Pentadinium membranaceum*, *Pentadinium sabulum* and *Pentadinium taeniagerum*, grano-bacculate in

Pentadinium laticinctum subsp. *granobaculatum*, verrucate in *Pentadinium lophophorum* or honeycombed in *Pentadinium favatum*. Furhermore, *Pentadinium darmirae* sp. nov. is limited to the lower–middle Danian interval, while all the other *Pentadinium* species listed for comparison are known only from younger Eocene and Miocene deposits.

Stratigraphic occurrence. Samples P164R–P170I (lower–middle Danian), Varniţa section, Tarcău Nappe; lower Danian of the Vrancea Nappe, Eastern Carpathians, Romania (Ţabără and Slimani, 2017).

8. Conclusions

Based on dinoflagellate cysts, planktonic and agglutinated foraminifera and calcareous nannofossils from the Varniţa section, an integrated biostratigraphy was established for the Upper Cretaceous–Paleogene succession of the northern Moldavidian Domain (Eastern Carpathians). Using palynofacies data and the agglutinated foraminiferal morphogroups, the depositional environments across the upper Maastrichtian to Danian sedimentary succession were assessed. The main conclusions are the following:

(1) The microfossil assemblages identified in the upper part of the Hangu Formation indicate a late Maastrichtian age for the deposits assigned to this formation. Important biostratigraphic events supporting the attribution are the FADs of *Nephrolithus frequens* and *Micula* cf. *prinsii* among the nannofossils, the FADs of *Cerodinium speciosum*, *Deflandrea galeata*, *Disphaerogena carposphaeropsis* and LADs of *Dinogymnium* spp., *Isabelidinium cooksoniae*, *Palynodinium grallator* (among the dinocysts) and the occurrence of the foraminifer *Abathomphalus mayaroensis*. An early Danian age of the deposits assigned to the Runcu Formation is suggested by the bloom of the calcareous dinoflagellate genus *Thoracosphaera* (samples P163R and P164R), as well as FADs of the *Xenicodinium lubricum* and *X. reticulatum* which allow correlation with lower Danian *Xenicodinium lubricum* Zonule (Hansen, 1977). The *Rzehakina fissistomata*, mainly recorded in the Paleocene deposits, also occurs in the Runcu Formation slightly above the first occurrence of the *Xenicodinium lubricum* dinocyst. The global Danian dinocyst markers *Damassadinium californicum* and *Senoniasphaera inornata* occur only in the analyzed lower part of the Izvor Formation. *Senoniasphaera inornata* suggests an early–middle Danian age (66–62.6 Ma) for this interval.

(2) *Pentadinium darmirae* sp. nov. is described from the Runcu and Izvor formations. This is the first record of the *Pentadinium* in the Paleocene. Almost all the other *Pentadinium* species are known from younger Eocene and Miocene deposits, except for *Pentadinium omasum* which occurs in the Barremian.

(3) The disappearance of the planktonic calcareous foraminifera due to carbonate dissolution, as well as a significant decrease in abundances of the benthic calcareous foraminifera and nannoplankton at the end of the Cretaceous was noted. In contrast, most of the dinocyst taxa and agglutinated foraminifera recorded in the upper Maastrichtian cross the K–Pg boundary and persist into the Danian.

(4) The upper Maastrichtian–Danian boundary lies somewhere within some 16 m thick interval between the top of the Hangu Formation (sample P162H) and the Runcu Formation (sample P163R), which is covered by a landslide. Moreover, a high accuracy location of the K–Pg boundary in the studied section is probably difficult to achieve, because this event may be synchronous with sedimentation of debris flow type of the Runcu Formation. The marker taxa defining the uppermost Maastrichtian zones (e.g. Subzone "b" of the dinocyst *Hystrichostrogylon coninckii* Zone) as well as the lowermost Danian dinocyst *Carpatella cornuta* Zonule, were not identified in the studied samples. We assume that these zones may be identified in the deposits hidden under the above mentioned landslide.

(5) The composition of POM, the agglutinated foraminiferal morphogroups and the C/M ratio identified in the upper Maastrichtian deposits (Hangu Formation) suggest an outer shelf to distal (bathyal) depositional environment for the interval. Anoxic conditions inside of microfossil tests allowed the crystallization of the framboidal pyrite identified in the Hangu Formation. A marine transgression during the deposition of the lower Danian sequence is supported by changes in the palynofacies composition and microfossil assemblages identified.

Acknowledgements

We are indebted to Prof. A. Gautier from the Research Unit Palaeontology of Ghent University for his helpful constructive review and improvement the English of the manuscript. The constructive reviews and thoughtful comments of the two anonymous reviewers and the associate editor M. Machalski are greatly appreciated.

References

van den Akker, T.J.H.A., Kaminski, M.A., Gradstein, F.M., Wood, J., 2000. Campanian to Palaeocene biostratigraphy and palaeoenvironments in the Foula Basin, west of Shetland Islands. Journal of Micropalaeontology 19, 23–43.

Alvarez, L.W., Alvarez, W., Asaro, F., Michel, H.V., 1980. Extraterrestrial cause for the Cretaceous–Tertiary extinction. Science 208, 1095–1108. http://dx.doi.org/10.1126/science.208.4448.1095.

Antonescu, E., Alexandrescu, G., 1979. Données préliminaires sur les dinoflagellés des couches de Hangu (Sénonien-Paléocène). Dări de Seamă ale Institutului de Geologie şi Geofizică 66, 61–93.

Bădescu, D., 2005. The tectonic and stratigraphic evolution of the East Carpathians during Mesozoic and Neozoic. Editura Economică, Bucureşti, 312 pp, (in Romanian).

Bąk, K., Wolska, A., 2005. Exotic orthogneiss pebbles from Paleocene flysch of the Dukla Nappe (Outer Western Carpathians, Poland). Geologica Carpathica 56 (3), 205–221.

Batten, D.J., 1999. Small palynomorphs. In: Jones, T.P., Rowe, N.P. (Eds.), Fossil Plants and Spores: Modern Techniques. Geological Society, London, pp. 15–19.

Bindiu, R., Filipescu, S., 2011. Agglutinated Foraminifera from the Northern Tarcău Nappe (Eastern Carpathians, Romania). Studia Universitatis Babeş-Bolyai, Geologia 56 (2), 31–41.

Bojar, A.V., Bojar, H.P., 2013. The Cretaceous–Paleogene boundary in the East Carpathians, Romania: evidence from geochemistry, mineralogy and calcareous nannofossils. In: Bojar, A.V., Melinte-Dobrinescu, M.C., Smit, J. (Eds.), Isotopic Studies in Cretaceous Research. Geological Society, London, pp. 105–122. http://dx.doi.org/10.1144/SP382.11. Special Publications 382.

Bojar, A.V., Melinte-Dobrinescu, M.C., Bojar, H.P., 2009. A continuous Cretaceous-Paleocene red-bed section in the Romanian Carpathians. In: Hu, X., Wang, C., Scott, R.W., Wagreich, M., Jansa, L. (Eds.), Cretaceous Oceanic Red Beds: Stratigraphy, Composition, Origins, and Paleoceanographic and Paleoclimatic Significance. SEPM, Special Publications 91, pp. 121–135.

Bombardiere, L., Gorin, G.E., 2000. Stratigraphical and lateral distribution of sedimentary organic matter in Upper Jurassic carbonates of SE France. Sedimentary Geology 132, 177–203. http://dx.doi.org/10.1016/S0037-0738(00)00006-3.

Brinkhuis, H., Zachariasse, J.W., 1988. Dinoflagelltes cysts, sea level changes and planktonic foraminifera across the Cretaceous–Tertiary boundary at El Haria, northwest Tunisia. Marine Micropaleontology 13, 153–191.

Burnett, J.A., 1998. Upper Cretaceous. In: Bown, P.R. (Ed.), Calcareous nannofossils biostratigraphy. British Micropaleontology Society Series. Chapman and Hall, London, pp. 132–199.

Canfield, D.E., Raiswell, R., 1991. Pyrite formation and fossil preservation. In: Allison, P.A., Briggs, D.E.G. (Eds.), Taphonomy: Releasing the Data Locked in the Fossil Record. Topics Geobiology 9, pp. 337–387.

Caron, M., 1985. Cretaceous planktonic foraminifera. In: Bolli, H.M., Saunders, J.B., Perch-Nielsen, K. (Eds.), Plankton Stratigraphy. Cambridge University Press, pp. 17–86.

Carvalho, M.A., Mendonça Filho, J.G., Menezes, T.R., 2006. Palynofacies and sequence stratigraphy of the Aptian–Albian of the Sergipe Basin, Brazil. Sedimentary Geology 192, 57–74. http://dx.doi.org/10.1016/j.sedgeo.2006.03.017.
Carvalho, M.A., Cabral Ramos, R.R., Crud, M.B., Witovisk, L., Kellner, A.W.A., Silva, H.P., Grillo, O.N., Riff, D., Romano, P.S.R., 2013. Palynofacies as indicators of paleoenvironmental changes in a Cretaceous succession from the Larsen Basin, James Ross Island, Antarctica. Sedimentary Geology 295, 53–66. http://dx.doi.org/10.1016/j.sedgeo.2013.08.002.
Cetean, C., Bălc, R., Kaminski, M.A., Filipescu, S., 2011. Integrated biostratigraphy and palaeoenvironments of an upper Santonian – upper Campanian succession from the southern part of the Eastern Carpathians, Romania. Cretaceous Research 32, 575–590. http://dx.doi.org/10.1016/j.cretres.2010.11.001.
Cieszkowski, M., Golonka, J., Waśkowska, A., 2012. An olistolith interpretation for the Paleocene Szydlowiec sandstones in the stratotype area (Outer Carpathians, Poland). Austrian Journal of Earth Sciences 105 (1), 240–247.
Coccioni, R., Marsili, A., 2007. The response of benthic foraminifera to the K–Pg boundary biotic crisis at Elles (northwestern Tunisia). Palaeogeography, Palaeoclimatology, Palaeoecology 255, 157–180. http://dx.doi.org/10.1016/j.palaeo.2007.02.046.
Corliss, B.H., 1985. Microhabitats of benthic foraminifera within deep-sea sediments. Nature 314, 435–438. http://dx.doi.org/10.1038/314435a0.
Courtillot, V., 1990. Deccan volcanism at the Cretaceous-Tertiary boundary: past climatic crises as a key to the future? Global and Planetary Change 89 (3), 291–299. http://dx.doi.org/10.1016/0921-8181(90)90025-8.
Courtillot, V., Besse, J., Vandamme, D., Jaeger, J.J., Montigny, R., 1986. Deccan trap volcanism as a cause of biologic extinctions at the Cretaceous–Tertiary boundary? Comptes Rendus de l'Académie des Sciences de Paris 303, 863–868.
Dastas, N.R., Chamberlain Jr., J.A., Garb, M.P., 2014. Cretaceous-Paleogene Dinoflagellate Biostratigraphy and the Age of the Clayton Formation, Southeastern Missouri, USA. Geosciences 4, 1–29.
Duringer, P., Doubinger, J., 1985. La palynology: un outil de characterisation des facies marins et continentaux a la limite Muschelkalk Supérieur–Lattenkohle. Science Géologie Bulletin Strasbourg 38, 19–34.
Federova, V.A., 1977. The significance of the combined use of microphytoplankton, spores, and pollen for differentiation of multi-facies sediments. In: Samoilovich, S.R., Timoshina, N.A. (Eds.), Questions of Phytostratigraphy 398. Trudy Neftyanoi nauchno-issledovatelskii geologorazvedochnyi Institut (VNIGRI), Leningrad, pp. 70–88 (in Russian).
Fensome, R.A., MacRae, R.A., Williams, G.L., 2008. DINOFLAJ2, Version 1. American Association of Stratigraphic Palynologists, Data Series no. 1. http://dinoflaj.smu.ca/wiki/Main_Page.
Fisher, I.S.J., 1986. Pyrite replacement of mollusc shells from the Lower Oxford Clay (Jurassic) of England. Sedimentology 33, 575–585.
Gasiński, M., Uchman, A., 2009. Latest Maastrichtian foraminiferal assemblages from the Husów region region (Skole Nappe, Outer Carpathians, Poland). Geologica Carpathica 60 (4), 283–294. http://dx.doi.org/10.2478/v10096-009-0020-5.
Gasiński, M., Olshtynska, A., Uchman, A., 2013. Late Maastrichtian foraminiferids and diatoms from the Polish Carpathians (Ropianka Formation, Skole nappe): a case study from the Chmielnik-Grabówka composite section. Acta Geologica Polonica 63 (4), 515–525. http://dx.doi.org/10.2478/agp-2013-0022.
Gedl, P., 2004. Dinoflagellate cyst record of the deep-sea Cretaceous-Tertiary boundary at Uzgrun, Carpathian Mountains, Czech Republic. In: Beaudoin, A.B., Head, M.J. (Eds.), The Palynology and Micropalaeontology of BoundariesGeological Society Special Publications 230, pp. 257–273. http://dx.doi.org/10.1144/GSL.SP.2004.230.01.13.
Gradstein, F.M., Berggren, W.A., 1981. Flysch-type agglutinated foraminifera and the Maastrichtian to Paleogene history of the Labrador and North Seas. Marine Micropaleontology 6, 211–268.
Gradstein, F.M., Ogg, J.G., Schmitz, M.D., Ogg, G.M. (Eds.), 2012. The Geologic Time Scale 2012. Elsevier. http://dx.doi.org/10.1016/B978-0-444-59425-9.00001-9, 1144 pp.
Grasu, C., Catană, C., Grinea, D., 1988. Carpathian flysch. Petrography and economic considerations. Editura Tehnică, 208 pp, (in Romanian).
Guédé, K.É., Slimani, H., Louwye, S., Asebriy, L., Toufiq, A., Ahmamou, M., Amrani, El, El Hassani, I.E., Zeli Bruno Digbehi, Z.B., 2014. Organic-walled dinoflagellate cysts from the Upper Cretaceous–lower Paleocene succession in the western External Rif, Morocco: new species and new biostratigraphic results. Geobios 47, 291–304. http://dx.doi.org/10.1016/j.geobios.2014.06.006.
Guerrera, F., Martín Martín, M., Martín-Pérez, J.A., Martín-Rojas, I., Miclăuş, C., Serrano, F., 2012. Tectonic control on the sedimentary record of the central Moldavidian Basin (Eastern Carpathians, Romania). Geologica Carpathica 63, 463–479. http://dx.doi.org/10.2478/v10096-012-0036-0.
Habib, D., 1982. Sedimentary supply origin of Cretaceous black-shales. In: Schlanger, S.O., Cita, M.B. (Eds.), Nature and Origin of Cretaceous Carbon-rich Facies. Academic Press, London, pp. 113–127.
Habib, D., Olsson, R.K., Liu, C., Moshkovitz, S., 1996. High resolution biostratigraphy of sea level low, biotic extinction, and chaotic sedimentation at the Cretaceous–Tertiary Boundary in Alabama, north of the Chicxulub Crater. In: Ryder, G., Fastovsky, D., Gartner, S. (Eds.), The Cretaceous–Tertiary Event and Other Catastrophes in Earth History. Geological Society Of America, Special Paper 307, pp. 243–252.
Hammer, Ø., Harper, D.A.T., 2006. Paleontological Data Analysis. Blackwell Publishing, Oxford, 351 pp.
Hammer, Ø., Harper, D.A.T., Ryan, P.D., 2001. PAST: paleontological Statistics Software Package for Education and Data Analysis. Palaeontologia Electronica 4 (1), 9 pp. http://palaeo-electronica.org/2001_1/past/issue1_01.htm.
Hansen, J.M., 1977. Dinoflagellate stratigraphy and echinoid distribution in Upper Maastrichtian and Danian deposits from Denmark. Bulletin of Geological Society of Denmark 26, 1–26.
Hardenbol, J., Thierry, J., Farley, M.B., Jacquin, Th., de Graciansky, P.C., Vail, P.R., 1998. Mesozoic and Cenozoic sequence chronostratigraphic framework of European basins. In: de Graciansky, P.C., Hardenbol, J., Jacquin, Th., Vail, P.R. (Eds.), Mesozoic-Cenozoic Sequence Stratigraphy of European Basins. SEPM Special Publication 60, pp. 3–13, 763–781, and chart supplements.
Head, M.J., 1994. Morphology and paleoenvironmental significance of the Cenozoic dinoflagellate genera *Habibacysta* and *Tectatodinium*. Micropaleontology 40 (4), 289–321. http://dx.doi.org/10.2307/1485937.
Hollis, C.J., 1996. Radiolarian faunal change through the Cretaceous–Tertiary transition of eastern Marlborough, New Zealand. In: MacLeod, N., Keller, G. (Eds.), Cretaceous–Tertiary Mass Extinctions: Biotic and Environmental Changes. W.W. Norton and Co., New York, London, pp. 173–204.
Ion, J., Antonescu, E., Micu, M., 1982. On the Paleocene of the Bistriţa Half-window (East Carpathians). Dări de seamă ale şedinţelor, Institutul Geologic şi Geofizică 69 (4), 117–136.
Ionesi, L., 1966. Contributions on the Cretaceous-Paleogene boundary from external flysch zone of the Eastern Carpathians. Analele Ştiinţifice ale Universităţii "Al. I. Cuza" Iaşi, sect. IIb, Geologie-Geografie 12 81–90 (in Romanian).
Ionesi, L., 1971. Paleogene flysch from the Moldova River Drainage Basin. Editura Academiei Române, Bucureşti, 250 pp, (in Romanian).
Ionesi, L., 1975. Limite Maestrichtien-Paléocène et Cuisien nummulitique dans le flysch de Bucovine. In: 14-th European Micropaleontological Colloquium, Micropaleontological Guide to the Mesozoic and Tertiary of the Romanian Carpathians, Published by the Institute of Geology and Geophysics, Bucharest, pp. 145–150.
Ionesi, L., 1997. Formation de Runcu des Nappes de Vrancea et de Tarcău. Analele Ştiinţifice ale Universităţii "Al. I. Cuza" Iaşi, Geologie 42–43 107–113.
Ionesi, L., Tocorjescu, M., 1968. Microfaunistic data on the Cretaceous-Paleogene boundary in the outer flysch from Moldova Valley basin. Analele Ştiinţifice ale Universităţii "Al. I. Cuza" Iaşi, sect. II, Geologie-Geografie 14 61–68 (in Romanian).
Jones, R.W., Charnock, M.A., 1985. "Morphogroups" of agglutinating foraminifera. Their life position and feeding habits and potential applicability in (paleo) ecological studies. Revue de Paleobiologie 4, 311–320.
Kaminski, M.A., Gradstein, F.M., 2005. Atlas of Paleogene cosmopolitan deepwater agglutinated foraminifera. Grzybowski Foundation Special Publication 10, 574 pp.
Kaminski, M.A., Setoyama, E., Cetean, C.G., 2010. the phanerozoic diversity of agglutinated foraminifera: origination and extinction rates. Acta Paleontologia Polonica 55 (3), 529–539. http://dx.doi.org/10.4202/app.2009.0090.
Kędzierski, M., Gasiński, M., Uchman, A., 2015. Last occurrence of *Abathomphalus mayaroensis* (Bolli) foraminiferid index of the Cretaceous-Paleogene boundary: the calcareous nannofossil proof. Geologica Carpathica 66 (3), 181–195. http://dx.doi.org/10.1515/geoca-2015-0019.
Keller, G., 2008. Cretaceous climate, volcanism, impacts, and biotic effects. Cretaceous Research 29 (5–6), 754–771. http://dx.doi.org/10.1016/j.cretres.2008.05.030.
Keller, G., Sahni, A., Bajpai, S., 2009. Deccan volcanism, the KT mass extinction and dinosaurs. Journal of Biosciences 34 (5), 709–728. http://dx.doi.org/10.1007/s12038-009-0059-6.
Kuhnt, W., Kaminski, M.A., Moullade, M., 1989. Late Cretaceous deep-water agglutinated foraminiferal assemblages from the North Atlantic and its marginal seas. Geologische Rundschau 78 (3), 1121–1140.
Lamolda, M.A., Melinte, M.C., Kaiho, K., 2005. Nannofloral extinction and survivorship across the C/T boundary at Caravaca, southeastern Spain. Palaeogeography, Palaeoclimatology, Palaeoecology 224, 27–52. http://dx.doi.org/10.1016/j.palaeo.2005.03.030.
M'Hamdi, A., Slimani, H., Ismail-Lattrache, K.B., Soussi, M., 2013. Biostratigraphie des kystes de dinoflagellés de la limite Crétacé–Paléogène à Ellès, Tunisie. Revue de Micropaléontologie 56, 27–42. http://dx.doi.org/10.1016/j.revmic.2012.12.001.
M'Hamdi, A., Slimani, H., Louwye, S., Soussi, M., Ben Ismail-Lattrache, K., Ben Ali, W., 2015. Les kystes de dinoflagellés et palynofaciès de la transition Maastrichtien–Danien du stratotype El kef (Tunisie). Comptes Rendus Palevol 14, 167–180. http://dx.doi.org/10.1016/j.crpv.2015.01.008.
Machalski, M., Vellekoop, J., Dubicka, Z., Peryt, D., Harasimiuk, M., 2016. Late Maastrichtian cephalopods, dinoflagellate cysts and foraminifera from the Cretaceouse–Paleogene succession at Lechówka, southeast Poland: stratigraphic and environmental implications. Cretaceous Research 57, 208–227. http://dx.doi.org/10.1016/j.cretres.2015.08.012.
Martini, E., 1971. Standard tertiary and Quaternary calcareous nannoplankton zonation. In: Farinacci, A. (Ed.), Proceedings II Planktonic Conference, Rome, 1970. Telao Scienza, Rome 2, pp. 739–785.
McNeil, D.H., 1990. Stratigraphy and paleoecology of the Eocene *Stellarima* Assemblage Zone (pyrite diatom steinkerns) in the Beaufort- Mackenzie Basin, Arctic Canada. Bulletin of Canadian Petroleum Geology 38, 17–27.
Melinte, M.C., Jipa, D., 2005. Campanian-Maastrichtian marine red beds in Romania: biostratigraphic and genetic significance. Cretaceous Research 26, 49–56. http://dx.doi.org/10.1016/j.cretres.2004.11.002.

Mendonça Filho, J.G., Carvalho, M.A., Menezes, T.R., 2002. Palinofácies. In: Dutra, T.L. (Ed.), Técnicas e Procedimentos para o Trabalho com Fósseis e Formas Modernas Comparativas. Unisinos, São Leopoldo, pp. 20–24.
Mohamed, O., Piller, W.E., Egger, H., 2013. Dinoflagellate cysts and palynofacies across the Cretaceous/Palaeogene boundary at the Neritic Waidach Section (Eastern Alps, Austria). Review of Palaeobotany and Palynology 190, 85–103. http://dx.doi.org/10.1016/j.revpalbo.2012.11.002.
Murray, J.W., 2006. Ecology and Applications of Benthic Foraminifera. Cambridge University Press, Cambridge. http://dx.doi.org/10.1017/CBO9780511535529, 426 pp.
Murray, J.W., Alve, E., Jones, B.W., 2011. A new look at modern agglutinated benthic foraminiferal morphogroups: their value in palaeoecological interpretation. Palaeogeography, Palaeoclimatology, Palaeoecology 309, 229–241. http://dx.doi.org/10.1016/j.palaeo.2011.06.006.
Nagy, J., Gradstein, F.M., Kaminski, M.A., Holbourn, A.E.L., 1995. Late Jurassic to Early Cretaceous foraminifera of Thakkhola, Nepal: paleoenvironments and description of new taxa. In: Kaminski, M.A., Geroch, S., Gasiński, M.A. (Eds.), Proceedings of the Fourth International Workshop on Agglutinated Foraminifera. Grzybowski Foundation Special Publication 3, pp. 181–209.
Ogg, J.G., Hinnov, L.A., Huang, C., 2012. Cretaceous. In: Gradstein, F.M., Ogg, J.G., Schmitz, M.D., Ogg, G.M. (Eds.), The Geologic Time Scale 2012. Elsevier, pp. 793–853. http://dx.doi.org/10.1016/B978-0-444-59425-9.00027-5.
Olaru, L., 1978. Research on the stratigraphic distribution of microflora in the Paleogene flysch between Bistriţa and Trotuş Valleys. Institut de Géologie et de Géophysique, Mémoires 27, 5–111 (In Romanian).
Olszewska, B., 1997. Foraminiferal biostratigraphy of the Polish Outer Carpathians: a record of basin geohistory. Annales Societatis Geologorum Poloniae 67, 325–337.
Oszczypko, N., Malata, E., Bąk, K., Kędzierski, M., Oszczypko-Clowes, M., 2005. Lithostratigraphy and Biostratigraphy of the Upper Albian–Lower/Middle Eocene flysch deposits in the Bystrica and Raèa subunits of the Magura Nappe (Beskid Wyspowyand Gorce Ranges, Poland). Annales Societatis Geologorum Poloniae 75, 27–69.
Paul, C.R.C., 2005. Interpreting bioevents: what exactly did happen to planktonic foraminifers across the Cretaceous-Tertiary boundary? Palaeogeography, Palaeoclimatology, Palaeoecology 224, 291–310. http://dx.doi.org/10.1016/j.palaeo.2005.03.038.
Pellaton, C., Gorin, G.E., 2005. The Miocene New Jersey passive margin as a model for the distribution of sedimentary organic matter in siliciclastic deposits. Journal of Sedimentary Research 75, 1011–1027. http://dx.doi.org/10.2110/jsr.2005.076.
Perch-Nielsen, K., 1985. Mesozoic calcareous nannofossils. In: Bolli, H.M., Saunders, J.B., Perch-Nielsen, K. (Eds.), Plankton stratigraphy. Cambridge University Press, Cambridge, pp. 329–426.
Pospichal, J.J., 1996. Cretaceous nannofossils and clastic sediments at the Cretaceous–Tertiary boundary, northeastern Mexico. Geology 24, 255–258.
Powell, A.J., 1992. Dinoflagellate cysts of the Tertiary System. In: Powell, A.J. (Ed.), A Stratigraphic Index of Dinoflagellate Cysts. Chapman and Hall, London, pp. 155–252.
Prauss, M.L., 2009. The K/Pg boundary at Brazos-River, Texas, USA – An approach by marine palynology. Palaeogeography, Palaeoclimatology, Palaeoecology 283, 195–215. http://dx.doi.org/10.1016/j.palaeo.2009.09.024.
Săndulescu, M., 1984. Geotectonics of Romania. Editura Tehnică, Bucureşti, 336 pp, (in Romanian).
Schallreuter, R., 1984. Framboidal pyrite in deep-sea sediments. Initial Reports Deep Sea Drilling Project 75, 875–891.
Schiebel, R., Barker, S., Lendt, R., Thomas, H., Bollmann, J., 2007. Planktic foraminiferal dissolution in the twilight zone. Deep Sea Research Part II: Topical Studies in Oceanography 54, 676–686. http://dx.doi.org/10.1016/j.dsr2.2007.01.009.
Schiøler, P., Wilson, G.J., 1993. Maastrichtian dinoflagellate zonation in the Dan Field, Danish North Sea. Review of Palaeobotany and Palynology 78, 321–351. http://dx.doi.org/10.1016/0034-6667(93)90070-B.
Seiglie, G.A., 1973. Pyritization in living foraminifers. Journal of Foraminiferal Research 3 (1), 1–6.
Setoyama, E., Kaminski, M.A., Tyszka, J., 2011. The Late Cretaceous-Early Paleocene palaeobathymetric trends in the southwestern Barents Sea – Palaeoenvironmental implications of benthic foraminiferal assemblage analysis. Palaeogeography, Palaeoclimatology, Palaeoecology 307, 44–58. http://dx.doi.org/10.1016/j.palaeo.2011.04.021.
Setoyama, E., Radmacher, W., Kaminski, M.A., Tyszka, J., 2013. Foraminiferal and palynological biostratigraphy and biofacies from a Santonian – Campanian submarine fan system in the Vøring basin (offshore Norway). Marine and Petroleum Geology 43, 396–408. http://dx.doi.org/10.1016/j.marpetgeo.2012.12.007.
Sissingh, W., 1977. Biostratigraphy of Cretaceous calcareous nannoplankton. Geologie en Mijnbouw 56, 37–65.
Slimani, H., 1995. Les dinokystes des craies du Campanien au Danien at Hallembaye et Turnhout (Belgique), et à Beutenaken (Pays-Bas): biostratigraphie et systématique. PhD thesis, Research Unit Palaeontology, Ghent University, Belgium, 461 pp.
Slimani, H., 2000. Nouvelle zonation aux kystes de dinoflagellés du Campanien au Danien dans le nord et l'est de la Belgique et dans le sud-est des Pays-Bas. Memoirs of the Geological Survey of Belgium 46, 1–88.
Slimani, H., 2001. Les kystes de dinoflagellés du Campanien au Danien dans la région de Maastricht (Belgique et Pays-Bas) et de Turnhout (Belgique): biozonation et corrélation avec d'autres régions en Europe occidentale. Geologica et Palaeontologica 35, 161–201.
Slimani, H., Toufiq, A., 2013. A Cretaceous-Palaeogene boundary geological site, revealed by planktic foraminifera and dinoflagellate cysts, at Ouled Haddou, eastern external Rif Chain, Morocco. Journal of African Earth Sciences 88, 38–52. http://dx.doi.org/10.1016/j.jafrearsci.2013.08.008.
Slimani, H., Louwye, S., Toufiq, A., Verniers, J., De Conink, J., 2008. New dinoflagellate cyst species from Cretaceous/Palaeogene boundary deposits at Ouled Haddou, south-eastern Rif, Morocco. Cretaceous Research 29, 329–344. http://dx.doi.org/10.1016/j.cretres.2007.06.003.
Slimani, H., Louwye, S., Toufiq, A., 2010. Dinoflagellate cysts from the Cretaceous–Palaeogene boundary at Ouled Haddou, southeastern Rif, Morocco: biostratigraphy, paleoenvironments and paleobiogeography. Palynology 34, 90–124. http://dx.doi.org/10.1080/01916121003629933.
Slimani, H., Louwye, S., Dusar, M., Lagrou, D., 2011. Connecting the Chalk Group of the Campine Basin to the dinoflagellate cyst biostratigraphy of the Campanian to Danian in the borehole Meer (northern Belgium). Netherlands Journal of Geosciences 90, 129–164.
Slimani, H., Guédé, K.É., Williams, G.L., Asebriy, L., Ahmamou, M., 2016. Campanian to Eocene dinoflagellate cyst biostratigraphy from the Tahar and Sekada sections at Arba Ayacha, western External Rif, Morocco. Review of Palaeobotany and Palynology 228, 26–46. http://dx.doi.org/10.1016/j.revpalbo.2016.01.003.
Smit, J., Romein, A.T.J., 1985. A sequence of events across the Cretaceous–Tertiary boundary. Earth and Planetary Science Letters 74, 155–170. http://dx.doi.org/10.1016/0012-821X(85)90019-6.
Steffen, D., Gorin, G., 1993. Palynofacies of the Upper Tithonian–Berriasian deep-sea carbonates in the Vocotian Trough (SE France). Bulletin Centres Recheches Exploration-Prodution Elf Aquitaine 17, 235–247.
Szczepanik, P., Sawłowicz, Z., Bąk, M., 2004. Pyrite framboids in pyritized Radiolarian skeletons (Mid-Cretaceous of the Pieniny Klippen Belt, Western Carpathians, Poland). Annales Societatis Geologorum Poloniae 74, 35–41.
Ţabără, D., Slimani, H., 2017. Dinoflagellate cysts and palynofacies across the Cretaceous-Paleogene boundary interval of the Vrancea Nappe (Eastern Carpathians, Romania). Geological Quarterly 61 (1), 39–52. http://dx.doi.org/10.7306/gq.1302.
Ţabără, D., Pacton, M., Makou, M., Chirilă, G., 2015. Palynofacies and geochemical analysis of Oligo-Miocene bituminous rocks from the Moldavidian Domain (Eastern Carpathians, Romania): implications for petroleum exploration. Review of Palaeobotany and Palynology 216, 101–122. http://dx.doi.org/10.1016/jsevpalbo.2015.02.002.
Thierstein, H.R., 1980. Selective dissolution of Late Cretaceous and Earliest Tertiary calcareous nannofossils: experimental evidence. Cretaceous Research 1, 165–176. http://dx.doi.org/10.1016/0195-6671(80)90023-3.
Tshakreen, S.O., Gasiński, M.A., 2004. Cretaceous-Paleogene boundary problem in Libya: the occurrence of the foraminiferal species *Abathomphalus mayaroensis* (Bolli) in the Western Sirt Basin. Geological Quarterly 48, 77–82.
Twitchett, R.J., 2006. The palaeoclimatology, palaeoecology and palaeoenvironmental analysis of mass extinction events. Palaeogeography, Palaeoclimatology, Palaeoecology 232, 190–213. http://dx.doi.org/10.1016/j.palaeo.2005.05.019.
Tyson, R.V., 1995. Sedimentary Organic Matter: Organic Facies and Palynofacies. Chapman and Hall, London, p. 615.
Uchman, A., 2004. Deep-sea trace fossils controlled by palaeo-oxygentaion and deposition: an example from the Lower Cretaceous dark flysch deposits of the Silesian Unit, Carpathians, Poland. Fossils and Strata 51, 39–57.
Vasilyeva, O.N., 2013. Paleogene dinocysts from the Eastern Caspian Depression (the Uspenskaya SP-1 well, Kazakhstan). Lithosphere 1, 102–127.
Vasilyeva, O.N., Musatov, V., 2012. The Paleogene Dinoflagellate Cyst and Nannoplankton Biostratigraphy of the Caspian Depression. In: Elitok, Ö. (Ed.), Stratigraphic Analysis of Layered Deposits. InTech, pp. 161–194.
Vellekoop, J., Smit, J., van de Schootbrugge, B., Weijers, J.W.H., Galeotti, S., Sinninghe Damsté, J.S., Brinkhuis, H., 2015. Palynological evidence for prolonged cooling along the Tunisian continental shelf following the K–Pg boundary impact. Palaeogeography, Palaeoclimatology, Palaeoecology 426, 216–228. http://dx.doi.org/10.1016/j.palaeo.2015.03.021.
Westerhold, T., Röhl, U., Raffi, I., Fornaciari, E., Monechi, S., Reale, V., Bowles, J., Evans, H., 2008. Astronomical calibration of the Paleocene time. Palaeogeography, Palaeoclimatology, Palaeoecology 257, 377–403. http://dx.doi.org/10.1016/j.palaeo.2007.09.016.
Williams, G.L., Brinkhuis, H., Pearce, M.A., Fensome, R.A., Weegink, J.W., 2004. Southern Ocean and global dinoflagellate cyst events compared: index events for the late Cretaceouse-Neogene. In: Exon, N.F., Kennett, J.P., Malone, M.J. (Eds.), Proceedings of the Ocean Drilling Program. Scientific Results 189, pp. 1–98.
Willumsen, P.S., 2011. Maastrichtian to Paleocene dinocysts from the Clarence Valley, South Island, New Zealand. Alcheringa: An Australasian Journal of Palaeontology 35 (2), 199–240. http://dx.doi.org/10.1080/03115518.2010.494484.
Yepes, O., 2001. Maastrichtian-Danian dinoflagellate cyst biostratigraphy and biogeography from two equatorial sections in Colombia and Venezuela. Palynology 25, 217–249.

Appendix A. Supplementary data

Supplementary data related to this article can be found at http://dx.doi.org/10.1016/j.cretres.2017.04.021.